Evolution of deepwater mixing and weathering inputs in the central Atlantic Ocean over the past 33 Myr

M. Frank, T. van de Flierdt,[1] and A. N. Halliday

Institute for Isotope Geology and Mineral Resources, Department of Earth Sciences, Eidgenössische Technische Hochschule Zurich, Zurich, Switzerland

P. W. Kubik

Paul Scherrer Institute, Institute for Particle Physics, Eidgenössische Technische Hochschule Zurich, Zurich, Switzerland

B. Hattendorf and D. Günther

Laboratory for Inorganic Chemistry, Eidgenössische Technische Hochschule Zurich, Zurich, Switzerland

[1]   The isotopic composition of Nd in present-day deep waters of the central and northeastern Atlantic Ocean is thought to fingerprint mixing of North Atlantic Deep Water with Antarctic Bottom Water. The central Atlantic Romanche and Vema Fracture Zones are considered the most important pathways for deep water exchange between the western and eastern Atlantic basins today. We present new Nd isotope records of the deepwater evolution in the fracture zones obtained from ferromanganese crusts, which are inconsistent with simple water mass mixing alone prior to 3 Ma and require additional inputs from other sources. The new Pb isotope time series from the fracture zones are inexplicable by simple mixing of North Atlantic Deep Water and Antarctic Bottom Water for the entire past 33 Myr. The distinct and relatively invariable Nd and Pb isotope records of deep waters in the fracture zones appear instead to have been controlled to a large extent by contributions from Saharan dust and the Orinoco/Amazon Rivers. Thus the previously observed similarity of Nd and Pb isotope time series from the western and eastern North Atlantic basins is better explainable by direct supply of Labrador Seawater to the eastern basin via a northern pathway rather than by advection of North Atlantic Deep Water via the Romanche and Vema Fracture Zones.   *INDEX TERMS:* 4267 Oceanography: General: Paleoceanography; 1050 Geochemistry: Marine geochemistry (4835, 4850); 4283 Oceanography: General: Water masses; *KEYWORDS:* radiogenic isotopes, fracture zones, North Atlantic Deep Water, Antarctic Bottom Water, Saharan dust, Labrador Sea Water

1.   Introduction

[2] The dissolved isotopic compositions of Sr, Os, Nd, Hf, and Pb in the ocean are controlled mainly by weathering of different types and ages of continental crust. The isotopic signals of these rocks are generally delivered to the oceans via eolian or riverine inputs, whereas hydrothermal inputs are only significant for Sr and Os. The elements Nd, Pb and Hf have oceanic residence times on the order of or shorter than the global mixing time of the ocean. Their isotopic compositions have thus been used to trace present and past ocean circulation as well as the influence of changes in weathering inputs into the oceans (see *Frank* [2002] for a recent review).

[3] Neodymium has an oceanic residence time of ∼600–2000 years [*Jeandel*, 1993; *Jeandel et al.*, 1995; *Tachikawa et al.*, 1999]. It has been demonstrated from analyses of seawater samples that newly formed North Atlantic Deep Water (NADW) has an ε_{Nd} value of −13.5 caused by weathering contributions from old Archean rocks [*Piepgras and Wasserburg*, 1982, 1987; *Jeandel*, 1993] (Nd isotope ratios are expressed as ε_{Nd} values, which denote the deviation of the measured $^{143}Nd/^{144}Nd$ ratio from the chondritic uniform reservoir CHUR (0.512638), multiplied by 10,000). In contrast, water masses originating in the Southern Ocean such as Antarctic Bottom Water (AABW) or Antarctic Intermediate Water (AAIW) have higher Nd isotope ratios (ε_{Nd} = −7 to −9) [*Piepgras and Wasserburg*, 1982; *Jeandel*, 1993; *Bertram and Elderfield*, 1993]. Their isotopic compositions are mainly a consequence of mixing between waters from the Atlantic and the Pacific. The latter have much higher ε_{Nd} (−3 to −5) due to dominating weathering inputs from young volcanic rocks [*Piepgras and*

_____

[1]Now at Lamont Doherty Earth Observatory, Columbia University, Palisades, New York, USA.
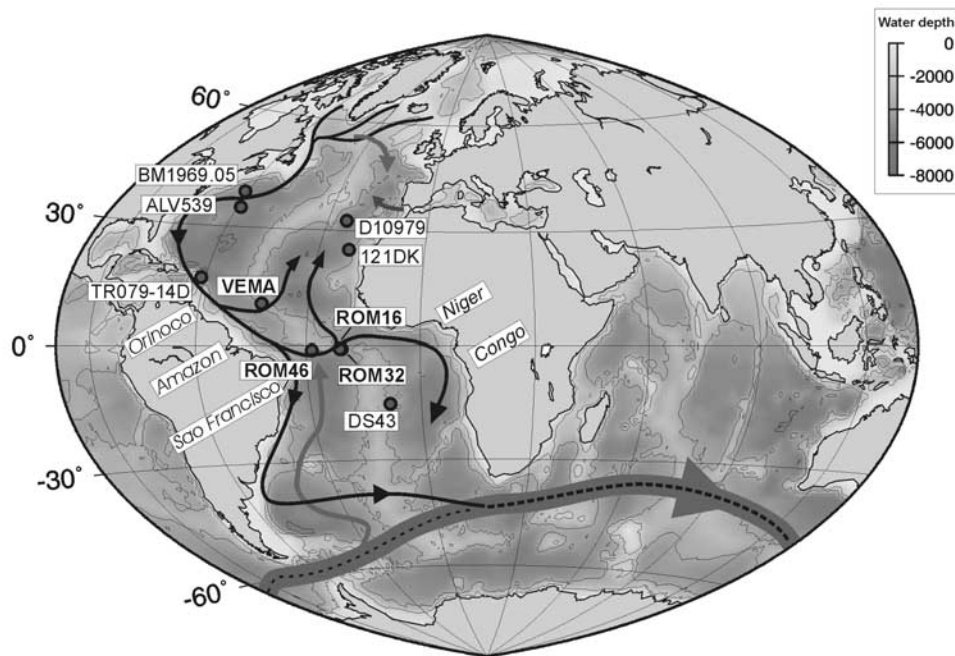
Figure 1. Locations of the investigated crusts of this study at the Romanche and Vema Fracture Zones and previously published records from the NW Atlantic Ocean, the northeastern Atlantic basin, and the Angola basin [*Burton et al.*, 1997, 1999; *O'Nions et al.*, 1998; *Abouchami et al.*, 1999; *Reynolds et al.*, 1999]. The flow pattern of NADW is shown schematically as a solid line. The circulation pattern of the ACC is given as a thick shaded line. The thinner shaded line leaving the ACC into the Argentine Basin stands for northward flowing LCDW (further downstream called AABW). Shaded arrows in the eastern North Atlantic denote MOW and middepth inflow of Labrador Seawater.

Jacobsen, 1988]. NADW is advecting south in the Atlantic Ocean and even at a latitude of 49°S the core of NADW at a depth of 2000 m is only slightly higher in ε_{Nd} (−12.5) than farther north [*Jeandel*, 1993]. This corroborates the quasi-conservative behavior of Nd in the western Atlantic Ocean despite potential effects of Saharan dust input and contributions of dissolved and particulate material from the Amazon and Orinoco Rivers. The distribution of Pb isotopes in the deep Atlantic ocean, as recorded by ferromanganese crust surfaces, has apparently also mainly been controlled by water mass distribution [*Abouchami and Goldstein*, 1995; *von Blanckenburg et al.*, 1996b]. However, Pb displays a more locally influenced isotopic distribution pattern as a consequence of its much shorter oceanic residence time, which is on the order of 50–100 years (see *Henderson and Maier-Reimer* [2002] for a recent compilation).

[4] The focus of this study are those branches of NADW which flow from the northwestern Atlantic into the eastern Atlantic basins through a number of gaps in the Mid-Atlantic Ridge, where vigorous vertical mixing with Antarctic Bottom Water (AABW) supplied from the South occurs [*Polzin et al.*, 1996; *Mercier and Morin*, 1997]. Volumetrically important are the deepest of these gaps, the Vema Fracture Zone (VFZ, ∼10°N), the Romanche Fracture Zone (RFZ, ∼0°), and the Chain Fracture Zone (CFZ, ∼2°S) (Figure 1). The estimated eastward deepwater flow of water colder than 1.9°C through the RFZ is ∼1.4 Sv (1 Sv = 10^6 m^3 s^{-1}) [*Mercier and Morin*, 1997]. For the VFZ ∼2–2.4 Sv of water colder than 2°C flowing eastward have been estimated [*McCartney et al.*, 1991; *Fischer et al.*, 1996], of which about 1.1 Sv are AABW [*Rhein et al.*, 1998]. The deep water derived from these through-flows has been claimed to be mainly responsible for the ventilation and renewal of deep waters in the northeastern and southeastern Atlantic Ocean basins [cf. *Broecker et al.*, 1985]. There is, however, also clear oceanographic evidence for a considerable flow (∼6 Sv) of western North Atlantic waters (Labrador Seawater - LSW) into the northeastern Atlantic at middepths (1500–2000 m) via a northern route [e.g., *Paillet et al.*, 1998; *Bower et al.*, 2002].

[5] There are no water column radiogenic isotope data from the RFZ and VFZ themselves but profiles in the western North and South Atlantic basins are available. These provide evidence that at present the Nd in the main body of NADW at a depth of about 2000 m is essentially undiluted (ε_{Nd} is still −13.5) by the time it reaches 7°N, just prior to entering the fracture zones [*Piepgras and Wasserburg*, 1987]. At this latitude at depths of 3000–4000 m, ε_{Nd} values between −12.4 and −12.8 indicate that NADW starts to show admixture of some portions of AABW from below. In contrast, the Nd isotope compo-

Table 1. Locations and Details of Crusts

Cruise	Sample	Name Used in Text	Latitude	Longitude	Water Depth, m	Thickness, mm	Average Growth Rate, mm/Myr	Base Age, Ma
ROM 96	G 9646-63	ROM46	01°12.5–13.5′S	28°32.3–30.9′W	3650–3050	85	2.6	33
ROM 96	G 9632-47	ROM32	00°48.9–51.2′S	21°01.3–00.2′W	5488–3933	16	3.2	5
ROM 96	S 1601-13	ROM16	00°48.2–48.5′S	20°35.8–35.7′W	3300–3100	15	5.5	2.7
VEMA CH78	DR01-001a	Vema	10°35.0′N	42°42.0′W	3512	21	4.95	4.2

sition of AABW itself at this location is already very strongly modified, mainly by mixing with NADW from above, and shows an ε_{Nd} value of −11.8. In the northeastern Atlantic the northward flowing branch of the waters derived from the Fracture Zones has been called eastern NADW (ENADW) and has ε_{Nd} values between −11.6 and −11.9 at a depth of 2500 m [*Tachikawa et al.*, 1999]. Nd isotope ratios of seawater from shallower depths (0–1100 m) at this and other neighboring sites in the northeastern Atlantic show more negative values (ε_{Nd} down to −13). This was interpreted as a contribution from partial dissolution of Saharan dust because the dust particles at the same sites and water depths have ε_{Nd} values between −12 and −14 [*Tachikawa et al.*, 1997]. For the deeper waters below at 2500 m depth, however, the dissolved Nd isotope signature can be explained without contributions from dust by mixing of western NADW with AABW in the Fracture Zones alone.

[6] Time series of the Nd, Pb, and Hf isotope evolution of water masses in the Atlantic Ocean have been obtained from ferromanganese crusts. For NADW or a precursor of it, significant changes of the signature of all three isotope systems over the past 3 Myr have mainly been related to the changes in weathering regime and erosional input associated with the onset of Northern Hemisphere glaciation (NHG) [*Burton et al.*, 1997, 1999; *O'Nions et al.*, 1998; *Reynolds et al.*, 1999; *von Blanckenburg and O'Nions*, 1999; *Piotrowski et al.*, 2000; *van de Flierdt et al.*, 2002]. The Nd isotope composition of NADW decreased by ∼2 ε_{Nd} units, mainly as a result of the increased supply of Nd with very negative ε_{Nd} from old continental crust in northern Canada and Greenland via LSW. This change was accompanied by a decrease in ε_{Hf} and changes in Pb isotope ratios caused by weathering old continental rocks under glacial conditions [*von Blanckenburg and Nägler*, 2001; *van de Flierdt et al.*, 2002]. Ferromanganese crust-derived Nd and Pb isotope time series of deep waters in the eastern North Atlantic Ocean show similar patterns over the past 4 Myr with a smaller amplitude, which has mainly been interpreted as a consequence of advection of NADW through the RFZ and VFZ, whereby the isotopic signal has been modified by mixing with water masses of southern origin [*Abouchami et al.*, 1999; *Reynolds et al.*, 1999]. It has, however, also been suggested recently that the Pb isotope time series of the eastern North Atlantic of the past few 100 kyr can not be explained only by water mass advection and mixing. Rather it was argued that there must have been a significant addition of Amazon or Orinoco-derived Pb to western

NADW before it enters the eastern basins [*Claude-Ivanaj et al.*, 2001].

[7] In this study we will reconstruct variations of North Atlantic interbasin water mass exchange and weathering inputs (riverine and eolian) by comparing four new ferromanganese crust time series from the Romanche and Vema Fracture Zones with time series in the western and eastern North Atlantic basins.

2. Material and Methods

[8] Three ferromanganese crusts from different water depths in the RFZ and one crust from the VFZ were analyzed in this study (Figure 1). Locations, sample depths and other details are given in Table 1. Three of the four crusts have been recovered from water depths between 3000 and 3650 m water depth corresponding to the present-day lower part of NADW, whereas at the greater depth (>3930 m) of crust G96-32-47 (called ROM32 below) larger proportions of AABW are present today [*Mercier and Morin*, 1997].

[9] The crusts were sampled continuously in 0.5–2.0 mm steps perpendicular to the macroscopically visible growth banding using a computer-controlled drill with a 10 mm diameter bit. Chemical separation and purification methods for Nd and Pb followed those of *Cohen et al.* [1988] and *Galer and O'Nions* [1989]. The Pb (applying a Tl-doping procedure [e.g., *Belshaw et al.*, 1998]) and Nd isotope measurements were performed on a Nu Instruments multiple collector inductively coupled plasma mass spectrometer (MC-ICPMS). $^{143}Nd/^{144}Nd$ was normalized to $^{146}Nd/^{144}Nd$ = 0.7219 to correct for instrumental mass bias. Age corrected $\varepsilon_{Nd(T)}$ values were calculated using $^{147}Sm/^{144}Nd$ = 0.115. All errors shown on the figures are 2σ external reproducibilities based on repeated measurements of standard materials. All ratios presented are normalized to given standard values: For JMC-Nd a given $^{143}Nd/^{144}Nd$ ratio of 0.511833, cross-calibrated to the La Jolla standard (0.511858) was used and for the NIST SRM981 Pb standard the ratios given by *Galer and Abouchami* [1998] were used for external normalization. The 2σ external precision for the Nd isotope measurements of the different sessions varied between 18 and 41 ppm, whereas the 2σ external precision of the Pb isotope measurements during different sessions was between 90 and 140 ppm for $^{206}Pb/^{204}Pb$, $^{207}Pb/^{204}Pb$, and $^{208}Pb/^{204}Pb$, between 20 and 60 ppm for $^{207}Pb/^{206}Pb$, and between 40 and 50 ppm for $^{208}Pb/^{206}Pb$. In run precision for each sample was better than the external reproducibility.

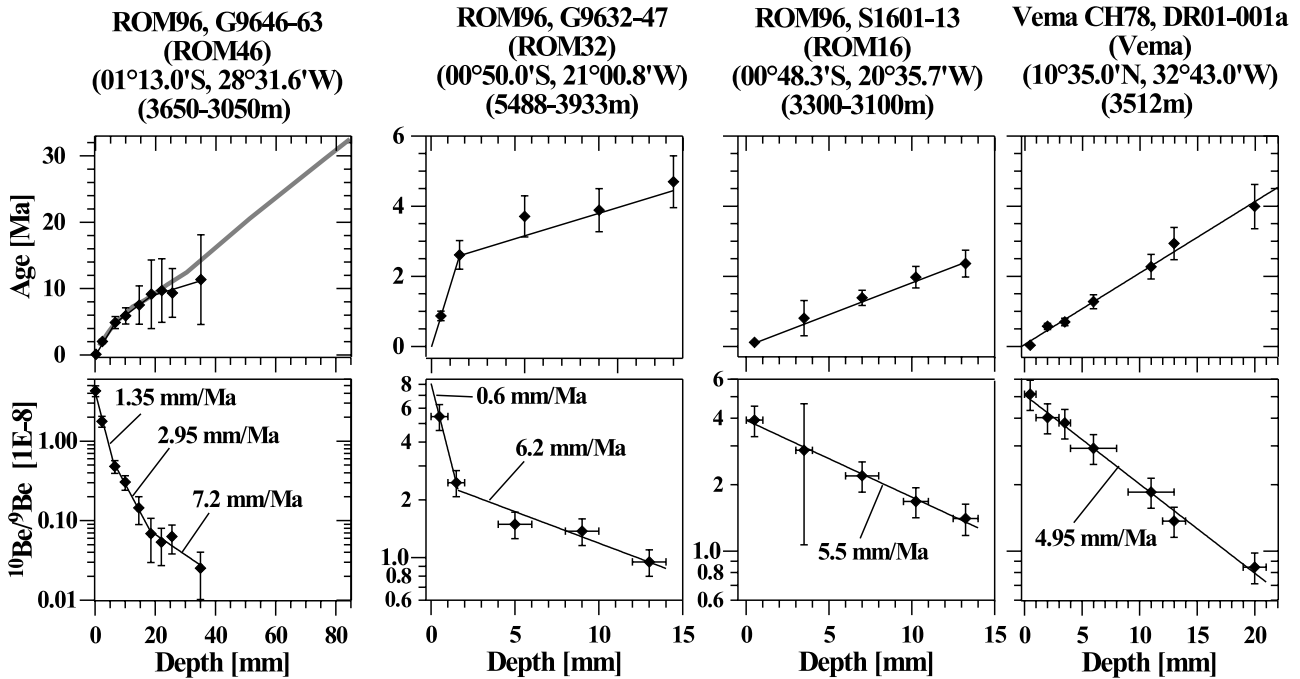**Figure 2.** Profiles of ^{10}Be/^{9}Be ratios for the four crusts from the Romanche and Vema Fracture Zones versus depth beneath the growth surface. The ages have been calculated with a half-life for ^{10}Be of 1.5 Ma and assuming a constant initial ^{10}Be/^{9}Be ratio. Note the different scales on the y axes. The growth rates and ages beyond the age range covered by ^{10}Be/^{9}Be data for crust ROM46 have been calculated using a Co-growth rate relationship [*Manheim*, 1986] which was forced to match the ^{10}Be/^{9}Be dating for the past 8.8 Myr (shaded line).

[10] Chemical preparation of the samples for the ^{10}Be AMS (Accelerator Mass Spectrometry) measurements followed closely a previously described method [*Henken-Mellies et al.*, 1990]. The samples of this study were measured at the Zurich AMS facility of the Paul Scherrer Institute and the ETH Zurich, Switzerland. The ^{10}Be concentrations were normalized to internal standard S555 with a nominal ^{10}Be/^{9}Be ratio of 95.5 × 10^{-12}. The 1σ statistical uncertainties of individual ^{10}Be measurements take into account both, the counting statistics of the ^{10}Be "events" and the reproducibility of repeated measurements, which were performed for each sample. The concentrations of ^{9}Be were measured, along with ^{59}Co, on the same aliquots by ICP-MS at the Laboratory of Inorganic Chemistry, ETH Zurich, Switzerland, using an ELAN 6100 DRC ICP-MS instrument. Rhodium and Ir were used as internal standards during calibration and analysis. Direct analysis of pressed powder pellets of the Nod A-1 ferromanganese crust standard by laser ablation ICP-MS [*Günther et al.*, 2000] at the Laboratory of Inorganic Chemistry reproduced the published data of *Axelsson et al.* [2002]. However, the data obtained by solution nebulization were offset by a constant amount. The reason for this discrepancy is unclear but a matrix effect is the most likely explanation. To correct for this, all solution measurements were normalized by comparing the measured and accepted values for Nod A-1 [*Axelsson et al.*, 2002]. Note that any such correction of the Be and Co concentration data by a constant factor does not influence the determination of the growth rates, and hence the age models. All data are available on

request from the corresponding author or electronically via the PANGAEA database.[1]

3. Results

[11] Generally, the concentration profiles of ^{10}Be show more scatter due to dilution effects than the ^{10}Be/^{9}Be profiles, which is the reason why only the results obtained from ^{10}Be/^{9}Be were considered reliable and were used to establish the age models (Table 2). The growth rates of the four crusts as derived from the ^{10}Be/^{9}Be profiles vary between 0.6 and 7.2 mm/Myr (Figure 2). For crusts S16-01-13 (called ROM16 below) and the one from the VFZ (called Vema below) no significant variations from a constant growth rate are obvious, whereas the ^{10}Be/^{9}Be data in the other two crusts are best explained by variable growth rates with a trend to lower growth rates in the younger parts. The difference in growth rate in ROM32 is derived from only two data points and has to be considered with some caution. However, its overall age is reliable given that the extrapolated ^{10}Be/^{9}Be ratio for zero age (0.80 × 10^{-7}) is consistent with expected values at this depth (see below). The age models used are displayed in Figure 2. Crust G96-46-63 (called ROM46 below) is the only one that extends

Table 2. Be Isotope and Co Concentration Data for the Four Crusts of This Study

Depth, mm	^{10}Be [× 10^8 atoms/g] ± 1σ SE	^{9}Be$_{measured}$, ppm	^{9}Be$_{corr.}$, ppm	^{10}Be/^{9}Be × 10^{-8} ± 1σ SE	Age, Ma	Co$_{measured}$, ppm	Co$_{corr.}$, ppm
			ROM96, G 9646-63 (ROM46)				
0.0–0.2	1.363 ± 0.059	2.7	4.7	4.300 ± 0.671	0.09 ± 0.01	2141	3404
2.0–2.5	1.256 ± 0.06	6.0	10.6	1.775 ± 0.280	2.03 ± 0.32	1530	2433
4.0–5.0	0.669 ± 0.052	-	-	-	-		
6.0–7.0	0.334 ± 0.035	5.9	10.4	0.482 ± 0.088	4.89 ± 0.89	1437	2285
9.5–10.5	0.218 ± 0.031	6.0	10.7	0.306 ± 0.063	5.89 ± 1.22	1579	2511
14.0–15.0	0.081 ± 0.029	4.8	8.4	0.145 ± 0.056	7.52 ± 2.89	1284	2042
18.0–19.0	0.040 ± 0.022	5.0	8.8	0.069 ± 0.039	9.17 ± 5.18	1427	2269
21.5–22.5	0.037 ± 0.017	5.8	10.3	0.054 ± 0.026	9.71 ± 4.78	1534	2439
25.0–26.0	0.044 ± 0.016	5.9	10.5	0.063 ± 0.025	9.35 ± 3.67	1406	2235
34.5–35.5	0.023 ± 0.013	7.6	13.4	0.025 ± 0.015	11.36 ± 6.76	1679	2670
67.0-68.0	< blank	5.5	9.7			1612	2564
84.0-85.0	< blank	2.8	5.0			1600	2544
			ROM96, G 9632-47 (ROM32)				
0.0-1.0	1.696 ± 0.051	2.6	4.7	5.438 ± 0.832	0.87 ± 0.13		
1.0-2.0	1.138 ± 0.047	3.9	6.9	2.459 ± 0.382	2.61 ± 0.41		
4.0-6.0	0.981 ± 0.048	5.6	9.8	1.491 ± 0.235	3.71 ± 0.59		
8.0-10.0	0.710 ± 0.034	4.4	7.7	1.373 ± 0.216	3.89 ± 0.61		
12.0-14.0	0.233 ± 0.011	2.1	3.7	0.950 ± 0.149	4.70 ± 0.74		
			ROM96, S 1601-13 (ROM16)				
0.0-1.0	1.324 ± 0.065	2.9	5.1	3.921 ± 0.619	0.12 ± 0.02		
3.0-4.0	2.156 ± 0.09	6.4	11.3	2.862 ± 1.793	0.81 ± 0.50		
6.0-8.0	1.336 ± 0.055	5.1	9.1	2.194 ± 0.341	1.39 ± 0.22		
9.5-11.0	1.218 ± 0.048	6.1	10.9	1.679 ± 0.260	1.98 ± 0.31		
12.5-14.0	0.913 ± 0.056	5.5	9.7	1.406 ± 0.228	2.36 ± 0.38		
			VEMA CH78, DR01-001a (Vema)				
0.0–1.0	2.656 ± 0.111	4.4	7.7	5.141 ± 0.801	0.04 ± 0.01		
1.0–3.0	2.601 ± 0.102	5.5	9.7	4.024 ± 0.624	0.57 ± 0.09		
3.0–4.0	2.284 ± 0.064	5.1	9.0	3.804 ± 0.580	0.70 ± 0.11		
4.0–8.0	1.903 ± 0.072	5.5	9.7	2.922 ± 0.452	1.28 ± 0.20		
8.0–9.0	1.824 ± 0.072	-	-	-	-		
9.0–13.0	1.418 ± 0.055	6.5	11.5	1.852 ± 0.287	2.27 ± 0.35		
12.0–14.0	1.058 ± 0.044	6.5	11.6	1.370 ± 0.213	2.94 ± 0.46		
19.0–21.0	0.637 ± 0.033	6.4	11.3	0.847 ± 0.134	3.99 ± 0.63		

beyond the maximum age datable with ^{10}Be/^{9}Be (~10 Ma). The lowermost four ^{10}Be/^{9}Be ratios in this crust in the depth range between 20 and 35 mm indicate a much higher growth rate of about 7.2 mm/Myr (Figure 2). The statistical uncertainties are, however, very large given that the ^{10}Be/^{9}Be ratios measured at the accelerator for these samples were close to those of the measurement blanks. In order to check whether this higher growth rate is realistic we compared the ^{10}Be/^{9}Be-derived growth rates with the results of a Co-constant flux model [*Manheim*, 1986; *Frank et al.*, 1999]. The growth rate calculation using the constant Co flux was forced to match the results of the ^{10}Be/^{9}Be-based model for the uppermost 20 mm (past 8.8 Myr) (Figure 2). There is no indication from these calculations for a change in growth rate for the period between 4.8 Ma and the base of the crust. We therefore applied this Co-based age model for the period older than 8.8 Myr in the following but it is noted that the uncertainties of the Co method are larger than those of the ^{10}Be/^{9}Be method. We will therefore not build any important conclusions on the exact timing of isotopic changes in the older part of this crust but only discuss the isotopic patterns.

[12] The surface ^{10}Be/^{9}Be ratios of the four crusts are uniform (between 0.39 to 0.54 × 10^{-7}) and in the range of previous results for North and central Atlantic crusts obtained by ion probe analyses in Oxford (ISOLAB) [*von Blanckenburg et al.*, 1996a; *Reynolds et al.*, 1999]. In particular, the surface value of crust Vema, which had been analyzed before by *von Blanckenburg et al.* [1996a], is identical within error (0.430 ± 0.035 compared with our value of 0.51 ± 0.08). The deepest crust (ROM32) shows the highest surface ^{10}Be/^{9}Be ratio (0.54 × 10^{-7}; extrapolated to zero age the value is 0.80 × 10^{-7}), consistent with a higher contribution of AABW with its ^{10}Be/^{9}Be ratio between 0.8 and 1 × 10^{-7} [*von Blanckenburg et al.*, 1996a; *Reynolds et al.*, 1999]. Water column ^{10}Be/^{9}Be results obtained by *Measures et al.* [1996] (station SAVE 158) for waters from a location further east and somewhat further south in the northern Angola Basin from the same depth as the RFZ crusts (3000–3600 m) are slightly higher than the RFZ data. This is consistent with efficient mixing of AABW and NADW in the Romanche and Chain Fracture Zones [*Polzin et al.*, 1996] (see below).

[13] The surface Nd and Pb isotope values for Vema and the two crusts from the RFZ that grew at water depths dominated by NADW at present, are similar within a very narrow range (Figure 3). The surface ε$_{Nd}$ values (−11.4 to −11.7) and ^{206}Pb/^{204}Pb (18.96 to 18.98) are in very good agreement with values of other crust surfaces in the

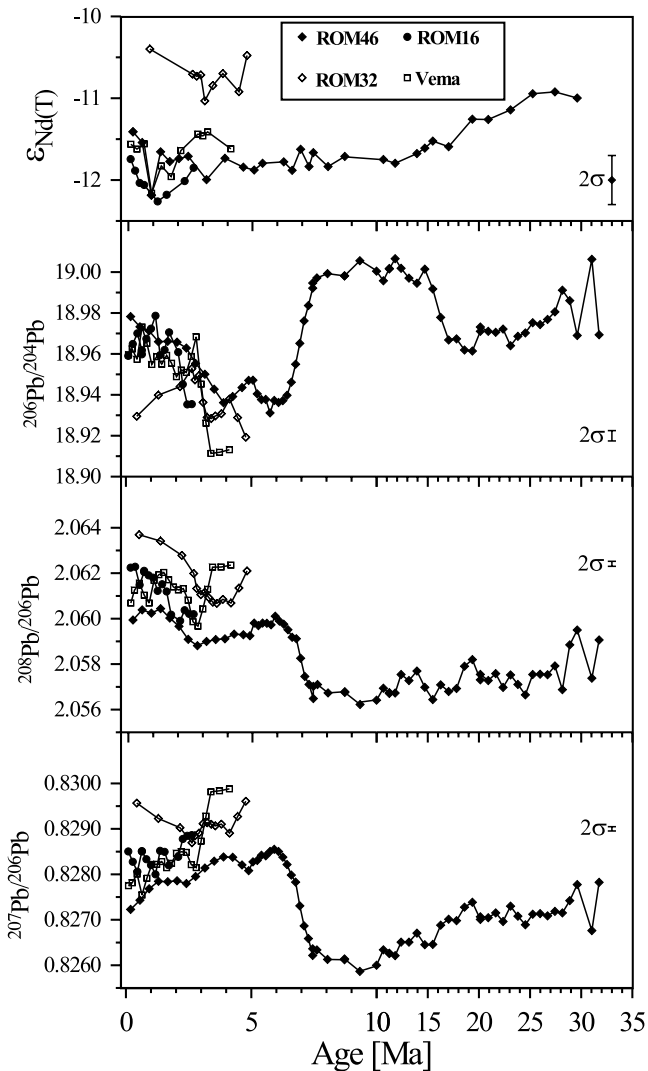**Figure 3.** Time series of $\varepsilon_{Nd(T)}$, $^{206}Pb/^{204}Pb$, $^{208}Pb/^{206}Pb$, and $^{207}Pb/^{206}Pb$ versus age for the four crusts from the Romanche and Vema Fracture Zones (ROM46, solid diamonds; ROM32, open diamonds; ROM16, solid circles; Vema, open squares). All error bars shown represent 2σ external reproducibilities of repeated standard measurements. Note the different scales for ages before and after 10 Ma.

equatorial Atlantic Ocean (see *Frank*, 2002 for a summary). In the case of Nd they also agree very well with water column measurements from the same depth in the tropical western and eastern Atlantic [*Piepgras and Wasserburg*, 1987; *Tachikawa et al.*, 1999]. The surface of the deepest crust (ROM32) shows somewhat different Pb isotope ratios and a significantly higher ε_{Nd} value (−10.5), which is again consistent with a higher proportion of admixed AABW with its typical ε_{Nd} values of −7 to −9 [*Piepgras and Wasserburg*, 1987; *Jeandel*, 1993].

[14] The most striking feature of the Nd isotope time series of the four crusts is that the composition has not varied strongly over the past 15 Myr. The only exception

appears to be a common trend to increase by half an ε_{Nd} unit between a minimum at about 1 Ma and the present, which is, however, barely outside statistical uncertainty of the measurements and will thus not be discussed further (Figure 3). Only prior to 25−30 Ma ε_{Nd} was as high as −11 and subsequently decreased to −11.7 at 15 Ma. This constancy is remarkable in view of the pronounced 2 ε_{Nd} negative shift observed for NADW in the western North Atlantic over the past 3 Myr [*Burton et al.*, 1997, 1999; *O'Nions et al.*, 1998] (Figure 4). The ε_{Nd} in deepest crust ROM32 has remained higher than the other three shallower crusts from the fracture zones by 1−1.5 ε_{Nd} units over the past 5 Myr. Thus the water column at the location of crusts ROM16 and ROM32 has obviously been vertically stratified in terms of Nd isotopes over this period. This provides evidence that vigorous mixing of AABW with overlying NADW observed for present-day waters further east in the RFZ [*Polzin et al.*, 1996] had not taken place at 21°W over the past 5 Myr, similar to the present oceanographic situation. Furthermore, the Nd isotope composition of the deep waters as recorded by the crusts can not have been controlled by leaching of or by pore water contributions from local deep sea sediments [*Grousset et al.*, 1988] since in this case the records ROM16 and ROM32 should show the same Nd isotope composition.

[15] Similar to Nd, the Pb isotope time series from the fracture zones show strikingly little variation over time compared with the other available North Atlantic time series (Figure 4). Nevertheless some clear patterns are resolvable (Figure 3). Between 5 Ma and present a significant increase in $^{206}Pb/^{204}Pb$ is observable in all three crusts from between 3000 and 3650 m water depth. The values range from 18.91 at 5 Ma to present-day values between 18.96 and 18.98. Over the same period of time the $^{207}Pb/^{206}Pb$ decreased. These patterns in Pb isotope ratios in the fracture zone time series are similar but of much smaller magnitude than the trends observed for crusts that have grown from NADW in the western North Atlantic [*Burton et al.*, 1997, 1999; *O'Nions et al.*, 1998; *Reynolds et al.*, 1999] and in the deep eastern North Atlantic [*Abouchami et al.*, 1999; *Reynolds et al.*, 1999] (Figure 4). In contrast, $^{208}Pb/^{206}Pb$ shows a slight increase over this period in the fracture zones whereas the other North Atlantic crusts show a pronounced decrease suggesting additional contributions of Pb at the fracture zones from different sources than at the other North Atlantic crust locations (see discussion). The Pb isotope ratios of deep crust ROM32 have differed from the other shallower crusts by showing slightly lower $^{206}Pb/^{204}Pb$ and higher $^{207}Pb/^{206}Pb$ ratios only over the past 2 Myr again pointing to an increased AABW contribution at this water depth (Figure 3). Between 7.3 and 6 Ma a distinct change in all Pb isotope ratios occurred in ROM46 whereas between the base of the crust at ∼33 Ma and 7.3 Ma all Pb isotope ratios have remained relatively constant, with the exception of an increase in $^{206}Pb/^{204}Pb$ from 18.96 to 19.0 between 17 and 15 Ma.

[16] Plotting the isotope time series of the fracture zone crusts in Pb-Pb isotope space reveals some distinct arrays despite the small range of variation (Figure 5). The time
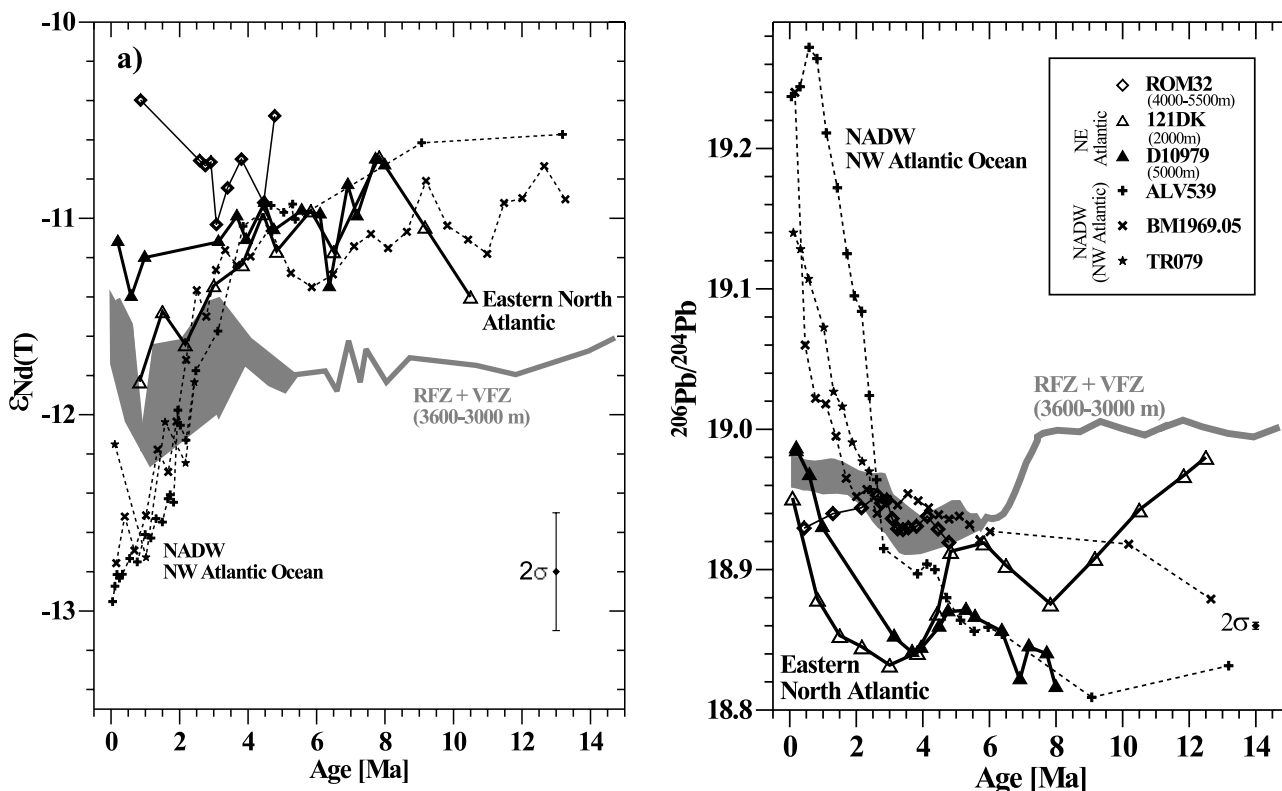
Figure 4. Comparison of (a) Nd and (b) ^{206}Pb/^{204}Pb time series of the western and eastern North Atlantic basins and the fracture zones for the past 15 Myr. The data for the three western North Atlantic crusts (ALV539, BM1969.05, and TR-079) are plotted as dashed lines [*Burton et al.*, 1997, 1999; *Reynolds et al.*, 1999], the ones from water depths of 3600-3000 m in the RFZ and VFZ are combined as shaded line/field, and the data from the deep RFZ (ROM32) are given as open diamonds and solid lines. The data for the eastern North Atlantic basin are given as open triangles and solid lines for crust 121DK [*Abouchami et al.*, 1999] and as solid triangles and solid lines for crust D10979 [*Reynolds et al.*, 1999].

periods comprised by these arrays coincide with the changes observed in the Pb isotope time series (Figure 3). The long time series of crust ROM46 can be subdivided into four clearly resolvable arrays in ^{208}Pb/^{204}Pb versus ^{206}Pb/^{204}Pb and ^{207}Pb/^{204}Pb versus ^{206}Pb/^{204}Pb space (0−2, 2−6.8, 6.8−27 and 27−33 Ma). These arrays may be interpreted as approximate binary mixing lines and show essentially identical slopes but are sometimes slightly offset relative to each other with respect to ^{206}Pb/^{204}Pb. This points to a prevailing control of two main end-members and either variable contributions of a third component that has remained relatively constant during the above periods or slight changes in the isotopic compositions of the end-members themselves. In ^{208}Pb/^{204}Pb versus ^{206}Pb/^{204}Pb space the arrays corresponding to the periods 2.0−6.8 and 27−33 Ma can be interpreted as binary mixture between the same end-members whereas in ^{207}Pb/^{204}Pb versus ^{206}Pb/^{204}Pb space this approximate "binary" array also includes the data for the period between 0 and 2 Ma.

[17] The Pb isotope data of the three other crusts are only slightly offset from the older parts of ROM46 toward higher ^{208}Pb/^{204}Pb and ^{207}Pb/^{204}Pb for a given ^{206}Pb/^{204}Pb (Figure 5). The data for the uppermost 2 Myr group closely together for all four crusts in Pb-Pb isotope

space and they are essentially indistinguishable in ^{208}Pb/^{204}Pb versus ^{206}Pb/^{204}Pb space (dark fields in Figure 5).

4. Discussion

[18] In order to reconstruct the history of water mass exchange through the Fracture Zones and to identify potentially important continental inputs, the Nd and Pb isotope compositions reported here will be compared with data for NADW in the western North Atlantic [*Burton et al.*, 1997, 1999; *O'Nions et al.*, 1998; *Reynolds et al.*, 1999], ENADW in the deep northeastern Atlantic basin [*Abouchami et al.*, 1999; *Reynolds et al.*, 1999], and AABW in the western Atlantic sector of the Southern Ocean [*Abouchami and Goldstein*, 1995; *Frank et al.*, 2002]. The deep southeastern Atlantic ocean has also been supplied by water masses derived from the RFZ and CFZ. It has previously been shown by *Reynolds et al.* [1999] that inputs from the Congo River have exerted a strong control, which prevents use of Nd and Pb isotopes in this basin as tracers for mixing of northern and southern water masses in the fracture zones. Note that the results achieved below represent the integrated glacial/
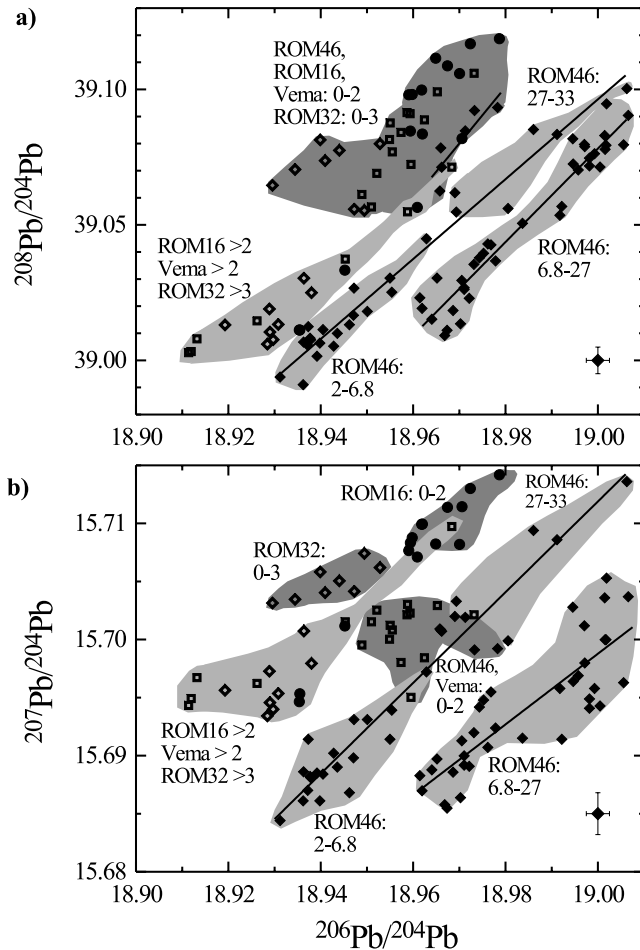
Figure 5. Comparison of Pb isotope composition of the crusts from the Romanche and Vema Fracture Zones in (a) $^{208}Pb/^{204}Pb$ versus $^{206}Pb/^{204}Pb$ and (b) $^{207}Pb/^{204}Pb$ versus $^{206}Pb/^{204}Pb$ space. Symbols are the same as in Figure 3. The numbers represent the ages (Ma) of the data within the distinct arrays. The uppermost 2 Myr are marked by dark shading, except for crust ROM32, where it marks the uppermost 3 Myr. The data corresponding to periods older than 2 Myr for ROM16 and Vema and older than 3 Myr for ROM32 form one array. The slopes (least squares fits) of the arrays of crust ROM46 are given as solid lines. Error bars represent 2σ external reproducibilities.

interglacial composition of the deep waters. Any potential changes in deepwater radiogenic isotope composition on glacial/interglacial timescales [*Rutberg et al.*, 2000; *Bayon et al.*, 2002] are not resolvable at the chosen sampling resolution.

4.1. Water Mass Mixing in the North Atlantic

[19] In Figures 4 and 6 the Nd and $^{206}Pb/^{204}Pb$ isotope evolutions of NADW and the eastern North Atlantic basin are compared with those of the Romanche and Vema Fracture Zones. For the most recent few 100 kyr, the Nd and Pb isotope data of the 3600–3000 m deep RFZ and

VFZ records have been very similar to the eastern North Atlantic data (121DK and D10979) [*Abouchami et al.*, 1999; *Reynolds et al.*, 1999; *Claude-Ivanaj et al.*, 2001]. This suggests that a major modification of the radiogenic isotope composition of NADW must have occurred already before NADW entered the fracture zones [*Claude-Ivanaj et al.*, 2001]. Over the past 3 Myr this situation has been entirely different. The 3600–3000 m Fracture Zone records of $^{206}Pb/^{204}Pb$ and Nd isotopes have apparently developed from a signature essentially identical to NADW at 2–3 Ma toward an isotopic signature that has only been similar to the eastern Atlantic records during the most recent few 100 kyr (Figure 4). This apparent evolution originates from the fact that all other North Atlantic records changed while the fracture zone records remained essentially constant.

[20] In the case of Nd isotopes this pattern is only consistent with water mass mixing between NADW and AABW if the export and thus the admixed proportion of NADW has progressively decreased over the past 2–3 Myr, as has been concluded from comparison of records of NADW with the Southern Ocean isotope evolution before [*Frank et al.*, 2002]. A persistently higher contribution of AABW compared with the other fracture zone records from depths of 3600–3000 m is documented by the Nd isotope record of deepest crust ROM32, which has remained distinctly more positive in its ε_{Nd} than all other deep North Atlantic crusts. The difference in Nd isotopes between the ROM32 record and NADW has increased continuously over the past 3 Myr, which is also in accordance with a progressive decrease of NADW contribution to the mixture of the waters in the deep RFZ. It is noted here that the observed patterns in the Nd isotope time series would also be consistent with a progressive decrease in the Nd concentration of NADW. There are, however, no data to support this and the fact that the increase in glacial erosion intensity in northern Canada and Greenland over the past 3 Myr has probably rather increased than decreased the Nd concentrations of NADW make this scenario very unlikely.

[21] The Nd isotope records of the fracture zones and the northeastern Atlantic basins prior to 3 Ma can not be explained at all by simple water mass mixing through the fracture zones. The Fracture Zone records were more negative in ε_{Nd} than both NADW and deep water in the eastern North Atlantic basin (Figure 4). However, for the time period covered by the eastern Atlantic crusts (12 to 3 Ma) the Nd isotope signatures of the records of the deep western and eastern North Atlantic were similar. Therefore a substantial part of the Nd in the deep waters filling the northeastern Atlantic basin may not have been advected within waters from the south through the fracture zones but may have been supplied via LSW and thus a northern pathway [*Paillet et al.*, 1998; *Bower et al.*, 2002] (see also section 4.2.3). Comparison of the oldest parts of the fracture zone records (15–33 Ma), covered only by crust ROM46, with the records from the western north Atlantic shows an indistinguishable Nd isotope composition (not displayed graphically) indicating either vigorous circulation or less isotopic differences in
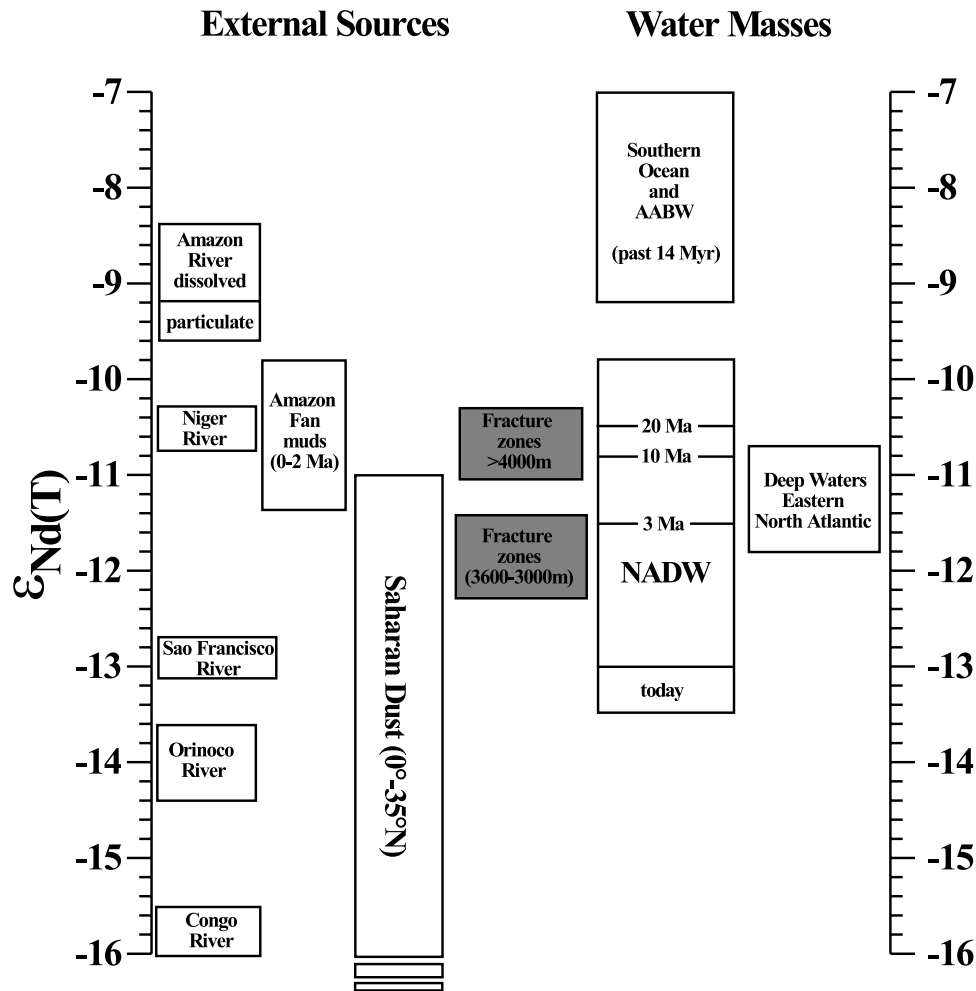
Figure 6. Comparison of the Nd isotope composition of potential external sources and water masses contributing to the isotope signature of the fracture zone crusts. References for the sources are included in the text.

weathering inputs to the Atlantic. The isotope compositions of Pb of the western North Atlantic and the RFZ were significantly different for the same period, consistent with its short oceanic residence time.

[22] At present, Pb isotope data representative for AABW in the western Atlantic sector of the Southern Ocean are only available for the past 3 Myr [*Abouchami and Goldstein*, 1995; *Frank et al.*, 2002]. We assume these, however, to be representative for at least the past 14 Myr due to the small range of variation observed for other Southern Ocean Pb isotope records during this period [*Frank et al.*, 2002]. Comparison of the AABW data with the other Atlantic records in Pb-Pb isotope space shows clearly that neither the fracture zone records nor the northeastern Atlantic records [*Abouchami et al.*, 1999; *Reynolds et al.*, 1999] can be explained by simple mixing of AABW and NADW at any time over the past 12 Myr (Figure 7). Lead must have been admixed from at least one additional source to explain the data. This may imply that additional sources have also contributed to the Nd isotope composition of the fracture zone waters over the past 3 Myr unless both isotope systems

have been decoupled. Such a decoupling has been found before for the central Indian Ocean [*Frank and O'Nions*, 1998] and more recently for the northernmost Pacific Ocean [*van de Flierdt et al.*, 2003; New constraints on the sources and behavior of neodymium and hafnium in seawater from Pacific Ocean ferromanganese crusts, submitted to *Geochimica Cosmochimica Acta*, 2003].

[23] The above results clearly show that there must have been additional sources of Nd (at least prior to 2−3 Ma) and Pb supplying the deep waters in the Fracture Zones with $\varepsilon_{Nd} < -12$ and $^{206}Pb/^{204}Pb > 19$. Riverine and/or eolian inputs must have been involved. In view of the low variability of the Nd and Pb isotope composition of the RFZ deep waters over the entire past 15 Myr, it appears likely that these external sources have also contributed to the Nd isotope signal over the past 3 Myr.

4.2. External Sources of Nd and Pb for Deep Waters in the Fracture Zone and the Northeastern Atlantic

[24] There are two major external sources of Nd and Pb that are likely to have contributed to the deep waters in the
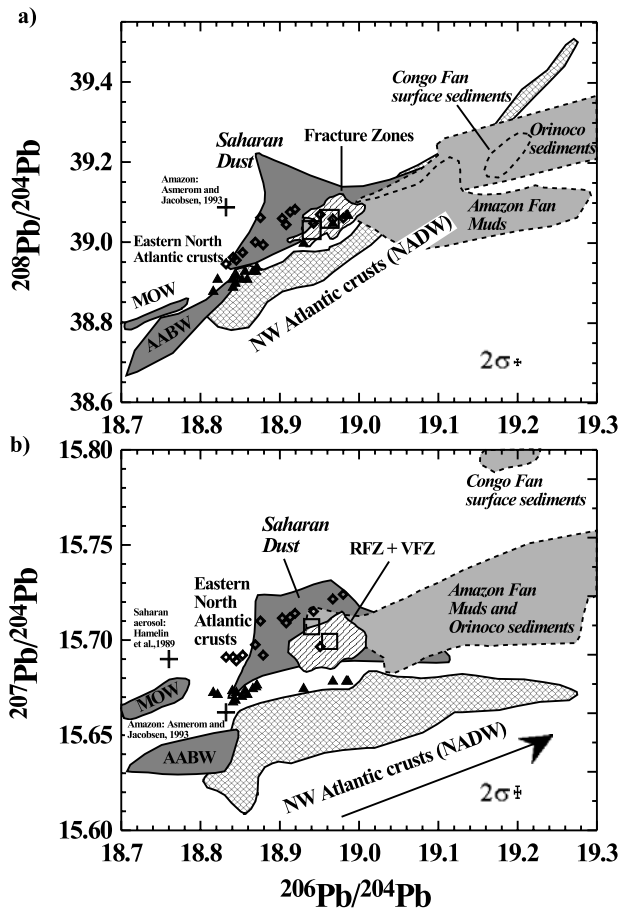
Figure 7. Comparison of Pb isotope composition of all central and north Atlantic crusts with potential external sources and water mass mixing end-members in (a) $^{208}Pb/^{204}Pb$ versus $^{206}Pb/^{204}Pb$ and (b) $^{207}Pb/^{204}Pb$ versus $^{206}Pb/^{204}Pb$ space. The crusts from the northwestern Atlantic [*Burton et al.*, 1997, 1999; *Reynolds et al.*, 1999] are marked as cross-stippled fields, and the stippled field corresponds to the crusts from the fracture zones. Data for northeastern crust 121DK [*Abouchami et al.*, 1999] are given as open diamonds and data for D10979 [*Reynolds et al.*, 1999] are given as solid triangles. The large open squares indicate the average composition of Amazon River material [*Allègre et al.*, 1996; this study]. The light shaded fields correspond to data for the Congo Fan, the Amazon Fan [*McDaniel et al.*, 1997], and Barbados and Demerara Abyssal Plain data [*White et al.*, 1985], the latter interpreted to represent Orinoco river particulates. One of the crosses marks a single data point for the Amazon Fan [*Asmerom and Jacobsen*, 1993] which is different from all other values and is therefore shown separately. The dark shaded fields represent sediment data from the North Atlantic ocean interpreted as Saharan dust [*Sun*, 1980], AABW (as obtained from ferromanganese nodule surfaces [*Abouchami and Goldstein*, 1995] and one time series [*Frank et al.*, 2002] from the western Atlantic sector of the Southern Ocean) and MOW [*Abouchami et al.*, 1999]. In Figure 7b a second cross marks one data point for a Saharan aerosol leach [*Hamelin et al.*, 1989] which is different from all other values and is therefore shown separately.

fracture zones and the eastern Atlantic basin over the past 33 Myr, which are (1) riverine inputs, most importantly from the Amazon and Orinoco, but potentially also from African rivers (Congo, Niger) and (2) detrital material of African origin (wind-blown dust from the Sahara) (Figures 6, 7, and 8).

4.2.1. Riverine Sources

[25] For the purpose of this study the Nd and Pb isotope compositions of the rivers are assumed to be identical to that of their suspended loads. This is justified for Nd isotopes [e.g., *Goldstein and Jacobsen*, 1987] but may have to be considered with some caution for Pb isotopes due to incongruent weathering effects [*von Blanckenburg and Nägler*, 2001].

4.2.1.1. Amazon River

[26] Present Amazon River material has ε_{Nd} values of −9.2 and −9.6 at the mouth of the river [*Goldstein et al.*, 1984]. Despite considerable Nd isotope variability of the suspended load of the Amazon tributaries, a value of −10.3, which is already very similar to the mouth, was found several hundred km upstream [*Allègre et al.*, 1996] indicating efficient homogenization. The dissolved signature at two stations was found to be essentially identical within error at ε_{Nd} of −8.4 and −9.2 [*Stordal and Wasserburg*, 1986], which is very similar to the signature of the suspended material. Over the past 2 Myr the Nd isotope composition of particulate Amazon River input into the Atlantic has been relatively invariant and overall slightly lower in ε_{Nd} (−11.4 to −9.8) as derived from analyses of Amazon Fan muds recovered during ODP Leg 155 [*McDaniel et al.*, 1997]. The Nd isotope signature of the Amazon River has thus been somewhat higher than the fracture zone records from 3600–3000 m water depth, at least over the past 2 Myr. Although there are no data on the Amazon River prior to 2 Ma, we can make the assumption that its Nd isotope signature has not changed dramatically over the past 10 Myr in view of the largely unchanged drainage pattern and tectonic setting [*Dobson et al.*, 1997]. Prior to 10 Ma the sedimentary inputs into the central Atlantic from South America have probably been smaller and significantly lower in ε_{Nd} due to a different prevailing drainage pattern [*Hoorn et al.*, 1995] and the preferential input of older Archean material derived from South American cratons such as the Guayana and Brasilian Shields, at least prior to 18 Ma [*Dobson et al.*, 1997]. The Amazon is a geologically relatively young feature as suggested from reconstruction of the continental drainage patterns [*Hoorn et al.*, 1995] and the age of the base of the Amazon Fan sediments of about 8–15 Ma [*Damuth and Kumar*, 1975]. Prior to that most of the water discharge was flowing north into the Caribbean causing smaller sedimentary supplies from the evolving Andean orogen (with its high Nd isotope values) to the Atlantic Ocean. However, the record of crust ROM46 shows significantly higher values prior to 15 Ma (Figure 3). In addition, an observed almost 10-fold increase in terrigenous sedimentation rates on Ceara Rise over the past 8 Myr, but most significantly over the past 3 Myr, which reflects Amazon river-derived material [*Dobson et al.*, 1997] did obviously not impact the Nd isotope evolution of the deep waters at the fracture zones, as
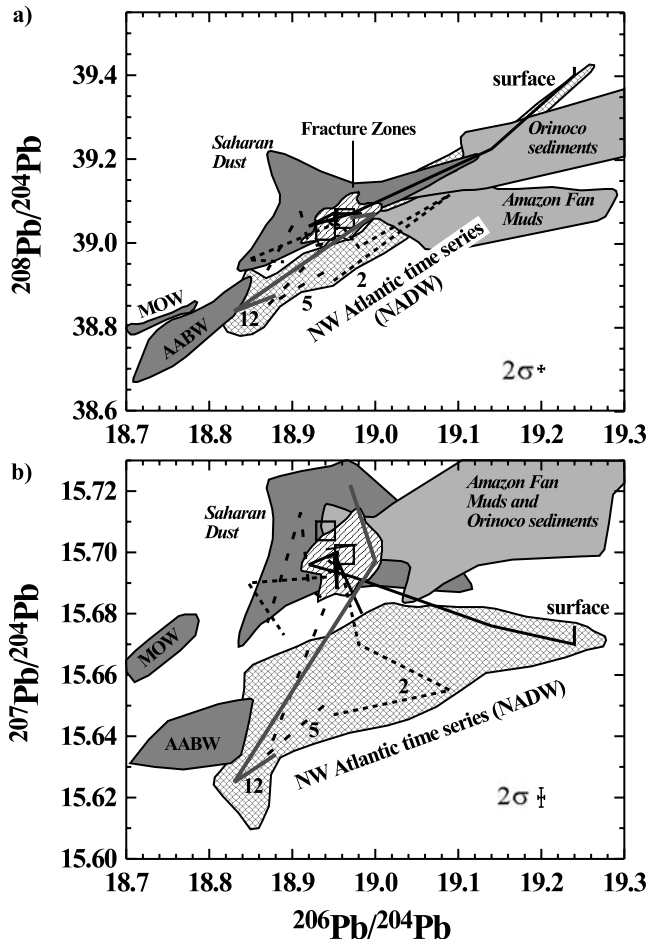
a)

b)

Figure 8. Time slice connections (surface, 2, 5, and 12 Ma) from the North Atlantic crusts in (a) ^{208}Pb/^{204}Pb versus ^{206}Pb/^{204}Pb and (b) ^{207}Pb/^{204}Pb versus ^{206}Pb/^{204}Pb space. Symbols and fields for all potential sources influencing the fracture zones are the same as in Figure 7. The lines mark connections between the data of particular time slices and are marked by numbers indicating the ages: surface, solid line; 2 Ma, thin dashed line; 5 Ma, thick dashed line; 12 Ma, dark shaded line.

documented by their invariable Nd isotope composition over the past 15 Myr. These lines of evidence suggest that Nd delivered by the Amazon River is not suitable to explain the Nd isotope evolution of the fracture zones over the past 33 Myr. Additional more negative sources (significantly below $\varepsilon_{Nd} = -12$) are required for the period between 15 and 3 Ma to produce ε_{Nd} values in the RFZ and VFZ which are as low as -12 (Figure 4).

[27] For Amazon River Pb, suspended particulate data [*Asmerom and Jacobsen*, 1993; *Allègre et al.*, 1996] and Amazon Fan surface sediments (analyzed during this study) indicate ^{206,207,208}Pb/^{204}Pb values of 18.83–18.96, 15.66–15.71, and 39.03–39.09, respectively (Figure 7). It is noted that the one least radiogenic value given by *Asmerom and Jacobsen* [1993] is very different from all other data and may either mean that this measurement is somehow anthro-

pogenically contaminated or that the other so far available and apparently tightly constrained data do not represent the entire range. Over the Pleistocene these Pb isotope values have generally been somewhat higher at 18.95–19.12, 15.68–15.72, and 38.99–39.20, respectively, as deduced from measurements of detrital material from the Amazon Fan of ODP Leg 155 [*McDaniel et al.*, 1997]. Thus the Pb isotope composition of the Amazon River particles (of the past 2 Myr) and the probably even more radiogenic signature of inputs prior to the major uplift of the Andes (~18 Ma [*Dobson et al.*, 1997]), render South American erosion products a suitable radiogenic end-member for the Pb in the RFZ and VFZ. Evidence from 55 Myr of near continuous terrigenous sedimentation on Ceara Rise directly adjacent to the present mouth of the Amazon [*Dobson et al.*, 1997] documents that erosional material from South America has been transported in the direction of the fracture zones. This reasoning requires either efficient scavenging of South America-derived dissolved Pb in the equatorial Atlantic as a means of vertical transport of the isotope signatures from the surface waters to the deep waters, or more likely, leaching of particulate material within the central Atlantic water column.

4.2.1.2. Orinoco River

[28] The present-day Nd isotope signal of the Orinoco River, as deduced from lower Orinoco sediments, is less radiogenic than the Amazon at $\varepsilon_{Nd} \sim -14$ [*Goldstein et al.*, 1997] and would thus be a suitable additional source of Nd. Geological evidence suggests that the Orinoco river (or its precursor) has probably existed since late Oligocene times, although it discharged into the Atlantic Ocean at a more northerly location than today [*Hoorn et al.*, 1995]. There is no direct information on the Pb isotope composition of the Orinoco River. *Claude-Ivanaj et al.* [2001] used the Pb isotope composition of the Barbados Ridge-Demerara Plain region [*White et al.*, 1985] to infer the Pb isotopic signal of the Orinoco River. The Amazon Fan Pb isotope data [*McDaniel et al.*, 1997] overlap with the Pb isotope composition of the Orinoco River obtained this way but the Orinoco data extend to somewhat higher ^{208}Pb/^{204}Pb and significantly higher ^{206}Pb/^{204}Pb and ^{207}Pb/^{204}Pb of up to 19.79 and 15.79, respectively. Lead supplied by the Orinoco would thus also be a suitable end-member for the fracture zone Pb (Figure 7).

[29] Orinoco River waters have mainly been transported northward into the Caribbean [*Müller-Karger et al.*, 1989] and probably have not turned around any more in the direction of the fracture zones over the past 20 Myr [e.g., *Nesbitt and Young*, 1997]. A viable mechanism by which Nd and Pb originating from the Orinoco River may nevertheless have reached the deep waters of the fracture zones is by vertical scavenging from the surface waters. The very low surface water Nd isotope ratios ($\varepsilon_{Nd} = -14$) in a present-day water column Nd isotope profile from 7°N were suggested to arise from dissolution of Saharan dust [*Piepgras and Wasserburg*, 1987]. They would, however, also be consistent with an Orinoco river source which may thus be considered a possible contributor of Nd for the fracture zone deep waters. There are no data on sedimentary records of Orinoco River discharge itself in the past but the

evolution of the drainage basin [*Hoorn et al.*, 1995] and sedimentary evidence from the Venezuelan Basin farther north [*Nesbitt and Young*, 1997] suggests that Orinoco River inputs, similar to the Amazon, were probably less radiogenic in Nd prior to about 15 Ma, which is inconsistent with the observed changes in the older part of ROM46.

[30] In Figure 7 the present-day Pb isotope signal of the Amazon and Orinoco Rivers is compared with the ferromanganese crust data and it is obvious that the values are very similar to the youngest parts of both the fracture zone records and the Eastern North Atlantic records. This suggests that Amazon/Orinoco river-derived Pb has strongly influenced the deepwater isotope composition in the fracture zones and thus also the deep eastern Atlantic over the past few 100 kyr [*Claude-Ivanaj et al.*, 2001]. This is further corroborated by a set of new Pb isotope data of the detrital fractions of sediments from the past 200 kyr from the Ceara Rise (western equatorial Atlantic) and the Sierra Leone Rise (eastern equatorial Atlantic). The detrital particles exhibit a narrow range of Pb isotope compositions, interpreted to be derived to a large extent from the Amazon/Orinoco Rivers and to some extent from Saharan dust [*Abouchami and Zabel*, 2003]. These data plot also almost exactly in the same range as the time series data for the fracture zone crusts and present-day Amazon, which supports the assumption that leaching of suspended particulates is the most important pathway of Amazon-derived Pb to the deep waters of the fracture zones.

[31] The situation prior to a few 100 ka was completely different, however. As can be seen from Figures 4 and 7, the Pb isotope data for the eastern North Atlantic and the Amazon and Orinoco particulates were distinctly different in the past. With age, they trend in opposite directions away from the composition of the fracture zones and the eastern North Atlantic over the past 3 Myr [*Abouchami et al.*, 1999] (Figure 7). This implies that the South American rivers contributed less to the dissolved Pb isotope composition of deep waters in the eastern North Atlantic prior to a few 100 ka, despite the inferred high particulate supplies over the entire past 4 Ma [*Dobson et al.*, 1997; *Nesbitt and Young*, 1997]. It is nevertheless possible that the Amazon and Orinoco have been mixing end-members for the Pb isotope composition of the fracture zone deep waters.

4.2.1.3. Sao Francisco River

[32] For the Sao Francisco River there are no Pb isotope data and the only available Nd isotope data point of particulate material also shows a relatively low ε_{Nd} value of −12.9 [*Goldstein et al.*, 1984]. Particulate material and surface water from this river is today transported northward by surface currents and may have reached the location of the RFZ [e.g., *Rühlemann et al.*, 2001], but it is unclear how important the contribution of such a relatively small river may have been.

4.2.1.4. African Rivers

[33] Comparison of the present-day Nd and Pb isotope composition of the most important African riverine source, the Congo River, with the isotope composition of the fracture zones shows that its present-day ε_{Nd} value of particulate Nd is between −15.5 and −16.1 [*Goldstein et al.*, 1984, *Allègre et al.*, 1996] also fits the requirement of a very unradiogenic Nd source. The amount of dissolved (colloidal) Nd supplied via the Congo is relatively high [*Dupré et al.*, 1996] and most of it is probably immobilized in the estuary, which together with the long transfer distance argues against the Congo River as an important source. If partial dissolution of the suspended material is, however, considered important it might be considered possible that it has contributed. We measured the Pb isotope composition of the clay fraction of Congo Fan surface sediments (below the bioturbation horizon to avoid anthropogenic bias). The data show a very radiogenic Pb isotope composition ($^{206,207,208}Pb/^{204}Pb$ values of 19.2, 15.79, and 39.2, respectively) which make the Congo an isotopically suitable contributor of Pb (Figure 7). There are today and probably have been in the past efficient surface currents from the Angola basin and the mouth of the Congo to the western equatorial Atlantic [e.g., *Peterson and Stramma*, 1991]. The long transport distance combined with the high particle reactivity of Pb strongly suggests, however, that the nearby sources have been much more important for Pb and probably also for Nd. The Niger River is an unlikely major supplier because its Nd isotope composition (−10.5 ε_{Nd}) [*Goldstein et al.*, 1984] is obviously not low enough to explain the isotope signal recorded by the fracture zone crusts.

[34] In summary, the isotopic compositions of both the Orinoco and the Amazon are suitable to increase the $^{206,207,208}Pb/^{204}Pb$ whereas only contributions from the Orinoco but not the Amazon are suitable to decrease the Nd isotope composition of the deep waters at the fracture zones if their isotopic compositions over the past 2 Myr are considered representative for their inputs over the past up to 15 Myr.

4.2.2. Eolian Sources

[35] The fracture zone crusts are located at the southern end of the present-day Saharan dust plume. The crust locations from the eastern North Atlantic Basin, particularly 121DK, have been located directly downwind of northwestern Africa within the Saharan dust plume [*Schütz*, 1980; *Prospero et al.*, 1981; *Rea*, 1994; *Romero et al.*, 1999; *Measures and Vink*, 2000; *Werner et al.*, 2002]. Therefore a contribution by dust to the radiogenic isotope composition of the deep waters is likely. This is particularly important because it has been suggested from measurements of seawater and particulate sediment trap material off West Africa that up to 20% of the Nd in dust particulates are dissolved releasing substantial amounts of REE to the surface waters [*Tachikawa et al.*, 1999]. Saharan dust, either directly collected or reconstructed from Late Quaternary marine sediments in the eastern North Atlantic between the equator and about 35°N has low ε_{Nd} values between −11 and −20 [*Goldstein et al.*, 1984; *Grousset et al.*, 1988, 1998; *Rognon et al.*, 1996; *Tachikawa et al.*, 1999] (Figure 6). In contrast, eastern Atlantic areas directly south of 0° obviously tend to receive dust material with higher ε_{Nd} values from different sources on the African continent. Areas north of 35°N also receive detrital material with higher ε_{Nd} values from other sources further north [*Goldstein et al.*, 1984; *Grousset et al.*, 1992, 1998]. Comparison of the Nd isotope composition of Saharan dust [*Grousset et al.*, 1998] with that of the fracture

zone records from 3600 to 3000 m water depth suggests that Saharan dust has been a suitable contributor of unradiogenic Nd in the past through partial dissolution of the dust particles in the surface waters and subsequent adsorptive transport to the deep waters. However, Saharan dust has not led to particularly low Nd isotope ratios in either the water column below 1500 m depth at locations directly underneath the present-day dust plume [*Tachikawa et al.*, 1999], or the crusts located directly under the plume (121DK) [*Abouchami et al.*, 1999]. If it is argued that detrital material and dust from Africa was the most likely candidate for contributing radiogenic Pb and unradiogenic Nd to the fracture zone deep waters but not to the deep eastern North Atlantic prior to 3 Ma, the only way to reconcile this apparent discrepancy is that the deep north eastern Atlantic received significant contributions from different deepwater sources compared with those at the fracture zones (see also next section).

[36] In the case of Pb the only available data points for present-day anthropogenically uncontaminated Saharan aerosols are very unradiogenic ($^{206}Pb/^{204}Pb$ = 18.76; $^{207}Pb/^{204}Pb$ = 15.69) [*Hamelin et al.*, 1989] More unpublished aerosol data of western Saharan (Mauretanian) origin, which are considered uncontaminated, show even lower $^{206}Pb/^{204}Pb$ ratios (below 18.4) which strongly points to a local unradiogenic Pb source (B. Hamelin, personal communication). This is supported by unradiogenic Pb isotope data on acid-leach residuals and preanthropogenic box core samples off Mauretania [*Hamelin et al.*, 1997]. In view of the large heterogeneity of Saharan rocks and the unradiogenic Nd isotope composition of the dust (see above), it is not likely that these data are representative for Saharan dust as a whole. Analogous to *Abouchami et al.* [1999], we therefore assume that the Pb isotope composition of northeastern Atlantic sediments corresponding to the aerial extent of the dust plume [*Sun*, 1980] is a more reliable representative for Saharan dust as a whole. The field inferred for Saharan dust in Figure 7 overlaps with most of the fracture zone data and most of those of crust 121DK [*Abouchami et al.*, 1999] suggesting that dust has been one of the main contributors of Pb as well. This is corroborated by the Pb isotope composition of detrital sediments from the Sierra Leone Rise in the eastern equatorial Atlantic, which apparently contains significant proportions of Saharan dust [*Abouchami and Zabel*, 2003] and which is very similar in its Pb isotope composition to that in the fracture zone crusts. Some of the data of these crusts and those of crust D10979 [*Reynolds et al.*, 1999] are offset from the north Atlantic sediment field toward lower $^{206,207,208}Pb/^{204}Pb$ values (Figure 7), which probably reflects the influence of NADW.

[37] It has been demonstrated from marine sedimentary records that the Saharan dust input into the North Atlantic has varied strongly in the past. In particular, it has been suggested from high accumulation rates of quartz and terrigenous sediments of particular grain sizes that the Sahara has only been a strong source of dust over the past 3–4 Myr and has not been an arid region comparable to today prior to that [e.g., *Tiedemann et al.*, 1989; *Rea*, 1994]. That suggests that dust has been less important prior to 4 Ma which is not mirrored in the Nd isotope time series and, if at all, in a small change of the Pb isotope time series of the

Table 3. Correlation Coefficients (r) Between Time Slice Pb Isotope Data[a]

Age, Ma	Number of Data Points to Correlate	$^{207}Pb/^{204}Pb$ Versus $^{206}Pb/^{204}Pb$	$^{208}Pb/^{204}Pb$ Versus $^{206}Pb/^{204}Pb$
Surface	9	**0.86**	**0.98**
1	9	0.54	**0.92**
2	9	0.43	**0.67**
3	9	0.05	0.50
4	7	0.21	0.21
5	6	0.28	0.50
8	5	0.40	0.73
12	4	0.91	**0.98**

[a]Those values of r which are significant at the 95% level are given in bold. The data for the surface, 2, 5, and 12 Ma are displayed graphically in Figure 8.

Fracture Zones (Figure 3), which, however, may also be explained by advection from the western Atlantic. Explanations for this apparent mismatch may be that the typical radiogenic isotope composition of the Saharan rocks has not only been delivered to the central Atlantic by dust, but also via rivers during the humid periods or that leaching of the West African shelf sediments played an important role similar to observations from the equatorial Pacific [*Lacan and Jeandel*, 2001].

4.2.3. Importance of the Sources of Nd and Pb Over Time for the Deepwater Isotope Signatures

[38] When comparing the deepwater Nd isotope composition reconstructed from the crust surfaces along the flow path of NADW, the increase of the Nd isotope ratios with distance from the sources in the north Atlantic are consistent with increasing admixture of a high-ε_{Nd} component such as AABW or Amazon-derived Nd. Further information can be gained from Pb. In order to investigate changes in source contributions to water masses in the Atlantic Ocean several studies have observed well-defined linear arrays of the time series data for single crusts in Pb-Pb isotope space which have been interpreted as binary mixing between two end-member sources of variable strength over certain periods of time [*Abouchami et al.*, 1999; *Reynolds et al.*, 1999; *Frank et al.*, 2002]. If, however, information on the mixing between different sources at one particular point in time in the ocean is to be acquired, the Pb isotope compositions at this particular point in time in the past from different crusts have to be compared. The nine Pb isotope time series now available from suitable locations allow such a comparison for the first time in the North Atlantic Ocean. Connected Pb isotope data for different time slices are plotted in Figure 8 (present, 2, 5, and 12 Ma). The correlations of all crust surfaces (representing the past few 100 kyr) result in well-defined binary mixing lines in both, $^{208}Pb/^{204}Pb$ versus $^{206}Pb/^{204}Pb$ and $^{207}Pb/^{204}Pb$ versus $^{206}Pb/^{204}Pb$ space, which is documented by correlation coefficients at a significance level better than 95% (Table 3). The mixing end-member on the radiogenic side is clearly NADW whereas for the unradiogenic end-member either Saharan dust or riverine Pb from the Amazon and Orinoco rivers (judging from the surface sediments of the Amazon fan and particulate data) or a combination of both would be suitable. From these connection lines it also

corroborated again that AABW cannot have provided any significant amounts of Pb to the equatorial Atlantic Ocean over the past few 100 kyr.

[39] Going back in time, it is again clear from the Nd isotope perspective that mixing of AABW and NADW can only explain the data back to 2–3 Ma if there was a strong reduction in NADW export. Prior to that additional external sources are required for the fracture zone locations. The most likely main source was Saharan material and possibly to some extent riverine inputs from the Orinoco. Given the constancy of the Nd and Pb isotope ratios it is probable that those sources have also been important for the fracture zones over the past 3 Myr. Thus the Nd isotope mixture in the deep waters of the fracture zones has probably also for the past 3 Myr not only been controlled by mixing of water masses but has also been influenced by external sources.

[40] In the case of Pb, it appears that Saharan dust and NADW have been the dominant end-members for the Pb isotopic mixture in the fracture zones together with some contribution from the South American rivers over at least the past 12 Myr (Figure 8). The connection lines between the Pb isotope data were significantly different prior to a few 100 ka and there are no more well-defined mixing lines which unambiguously points to the involvement of the above three or more local sources and which corroborates our earlier conclusion that mixing of only two water masses alone cannot explain the Pb isotope evolution of the fracture zones and the eastern North Atlantic. This is the case in particular for the periods between 2 and 8 Ma, where there was no significant correlation at all between the data points (Table 3). The main driving force for the observed changes in the positions and slopes of the connection lines has obviously been the pronounced Pb isotope evolution of NADW and to a lesser extent that of ENADW. The fact that essentially all connection lines of the 9 locations extend between the fields of NADW and Saharan dust and that some of the fracture zone data are extending below the field of Saharan dust in Figure 7 strongly suggests that NADW and Saharan dust have always been the main contributing sources of Pb in the fracture zones in the past. The inputs of other sources such as the Orinoco and Amazon rivers are superimposed but have apparently not dominated. If one considers the unlikely possibility that NADW has not been an important contributor of Pb in the past one could explain the fracture zone Pb isotope data also by mixing of Pb only derived from the Amazon/Orinoco and Saharan dust or even MOW.

[41] The Pb isotope composition of ENADW has obviously been controlled by different sources [see *Abouchami et al.*, 1999] but has mostly been within the fields for Saharan dust as derived from North Atlantic sediments. Some of the northeastern Atlantic data are outside the area that can be explained by mixing of NADW with dust or riverine-derived material. This may be due to incomplete data sets defining the arrays for the rivers and particularly for the Saharan dust, which may have to be extended toward less radiogenic Pb isotope ratios (see data of *Hamelin et al.* [1989]). Alternatively and more likely a fourth source may have been more important in the past, which is MOW (Figures 7, 8), the isotopic signature of which has been dominated largely by

Saharan dust and plots close to available Saharan aerosol data [*Hamelin et al.*, 1989]. This is consistent with the trends observed in the radiogenic isotope time series from the eastern North Atlantic [*Abouchami et al.*, 1999] and also with the estimate that MOW-derived Nd today equates to about 30% of the northern latitude-sourced Nd inputs into the North Atlantic [*Spivack and Wasserburg*, 1988]. That contribution by MOW may have even been higher in the past.

[42] This would further suggest that an efficient exchange of western North Atlantic-derived Nd and to some extent Pb with the northeastern Atlantic Ocean did not mainly occur via NADW through the fracture zones, at least prior to 3 Ma, but may have happened through pathways further north [*Paillet et al.*, 1998; *Abouchami et al.*, 1999; *Bower et al.*, 2002]. Such northern pathways in the present-day North Atlantic are again gaps in the Mid Atlantic Ridge at latitudes between 50° and 53°N such as the Charlie-Gibbs fracture zone and to a lesser extent the Faraday fracture zone [*Bower et al.*, 2002]. This is entirely consistent with the similarity of the Nd isotope compositions of NADW and ENADW prior to 3 Ma, which are clearly distinct from the fracture zone records. The main water mass having supplied the eastern north Atlantic Basin at middepths (1500–2000 m) via northern pathways is LSW. The changes in the Nd isotope composition of NADW over the past 3 Myr are mainly a reflection of large changes in the isotope composition of the LSW [*Vance and Burton*, 1999], which is one of the main components of NADW. A direct export of LSW or a water mass of similar origin to the eastern North Atlantic is in our opinion the most likely explanation for the similarity of the isotopic evolution of Nd and to a lesser extent of Pb in the eastern and western North Atlantic basins over the entire period of time covered by the crusts of this study.

5. Conclusions

[43] NADW and AABW in the Romanche Fracture Zone have been clearly distinguishable over the past 5 Myr at 21°W as shown by the persistently higher Nd isotope composition of the deepest crust below 4000 m compared with those at 3600–3000 m. This deep Nd isotope signal must reflect a higher proportion of AABW in agreement with present-day oceanographic results and excludes a control of the Nd isotope records by contributions from pore waters of the deep sea sediments.

[44] When comparing the NADW time series of Nd and Pb isotopes with the Fracture Zone records and those obtained in the eastern North Atlantic, it is clear that the Pb isotopes at no point in time can be solely explained by mixing of NADW and AABW. In the case of Nd isotopes the data for the past ~3 Myr are consistent with advection and mixing of NADW and AABW through the fracture zones into the eastern North Atlantic. If water mass mixing has indeed been the main controlling factor the Nd isotope patterns can only be explained by a drastic decrease in the contribution of NADW to the mixture of waters in the Fracture Zones over the past 2–3 Myr. Prior to that the radiogenic isotope composition of the deepwater masses

in the fracture zones must have received additional contributions from sources with very unradiogenic Nd and relatively radiogenic Pb. Given the remarkable constancy of the fracture zone records it is likely these sources have also contributed over the past 2–3 Myr, which probably prevents the use of Nd isotopes obtained from ferromanganese crusts in the central Atlantic Ocean as a stand alone quantitative tool to reconstruct changes of circulation and water mass mixing in the central Atlantic Ocean.

[45] Material from the Sahara (dust) has likely been the most important additional source for both, Nd and Pb in the fracture zones. If the Pleistocene range of Nd and Pb isotope data from the Amazon Fan is considered representative further back in time, then its ε_{Nd} has been slightly too high to be the additional source for the fracture zone deep waters and also Pb has at least not dominated the fracture zone records as indicated by Pb-Pb isotope relationships. The Orinoco River is a suitable source given its very low Nd isotope ratio and highly radiogenic $^{206,207,208}Pb/^{204}Pb$ ratios and may have contributed in varying proportions. A missing reflection of the drastic increase in riverine particulate discharge starting at ~4 Ma in the fracture zone records again limits the importance of the rivers. Comparison of the isotopic evolution of the deep waters in the fracture zones, at least prior to 3 Ma, with the distinct time series in the western and eastern North Atlantic suggests that the isotopic composition of the deep eastern North Atlantic has been strongly influenced by direct supply of Labrador Seawater via a northern route. In addition, Mediterranean outflow water may have played a more important role in the past for the radiogenic isotope composition of the deep waters of the eastern North Atlantic basin.

[46] In summary, the Nd and Pb isotope records from the Romanche and Vema Fracture Zones show that the use of radiogenic isotope records of dissolved seawater as independent large-scale proxy tracers for water mass mixing may be complicated by eolian or riverine inputs in the vicinity of significant such sources. Dust and probably also large rivers have contributed to the deep-water isotope composition of the fracture zones, most likely by partial dissolution of particulates, although the exact input and transfer mechanisms are not clear, mostly due to a lack of data. It is clear that more process studies and data are needed to further investigate the mechanisms by which trace metals are introduced and distributed in the ocean.

References

Abouchami, W., and S. L. Goldstein, A lead isotopic study of circum-Antarctic manganese nodules, *Geochim. Cosmochim. Acta*, 59, 1809–1820, 1995.

Abouchami, W., and M. Zabel, Climate forcing of the Pb isotope record of terrigenous input into the equatorial Atlantic, *Earth Planet. Sci. Lett.*, 213, 221–234, 2003.

Abouchami, W., S. J. G. Galer, and A. Koschinsky, Pb and Nd isotopes in NE Atlantic Fe-Mn crusts: Proxies for trace metal paleosources and paleocean circulation, *Geochim. Cosmochim. Acta*, 63, 1489–1505, 1999.

Allègre, C. J., B. Dupré, P. Négrel, and J. Gaillardet, Sr-Nd-Pb isotope systematics in Amazon and Congo River systems: Constraints about erosion processes, *Chem. Geol.*, 131, 93–112, 1996.

Asmerom, Y., and S. B. Jacobsen, The Pb isotopic evolution of the Earth: Inferences from river water suspended loads, *Earth Planet. Sci. Lett.*, 115, 245–256, 1993.

Axelsson, M. D., I. Rodushkin, J. Ingri, and B. Öhlander, Multielemental analysis of Mn-Fe nodules by ICP-MS: Optimisation of analytical method, *Analyst*, 127, 76–82, 2002.

Bayon, G., C. R. German, R. M. Boella, J. A. Milton, R. N. Taylor, and R. W. Nesbitt, An improved method for extracting marine sediment fractions and its application to Sr and Nd isotopic analysis, *Chem. Geol*, 187, 179–199, 2002.

Belshaw, N. S., P. A. Freedman, R. K. O'Nions, M. Frank, and Y. Guo, A new variable dispersion double-focussing plasma mass spectrometer with performance illustrated for Pb-isotopes, *Int. J. Mass. Spectrom.*, 181, 51–58, 1998.

Bertram, C. J., and H. Elderfield, The geochemical balance of the rare earth elements and neodymium isotopes in the oceans, *Geochim. Cosmochim. Acta*, 57, 1957–1986, 1993.

Bower, A. S., B. Le Cann, T. Rossby, W. Zenk, J. Gould, K. Speer, P. L. Richardson, M. D. Prater, and H.-M. Zhang, Directly measured mid-depth circulation in the northeastern North Atlantic Ocean, *Nature*, 419, 603–607, 2002.

Broecker, W. S., C. Rooth, and T.-H. Peng, Ventilation of the deep northeastern Atlantic, *J. Geophys. Res.*, 90, 6940–6944, 1985.

Burton, K. W., H.-F. Ling, and R. K. O'Nions, Closure of the Central American Isthmus and its effect on deep-water formation in the North-Atlantic, *Nature*, 386, 382–385, 1997.

Burton, K. W., D.-C. Lee, J. N. Christensen, A. N. Halliday, and J. R. Hein, Actual timing of neodymium isotopic variations recorded by Fe-Mn crusts in the western North Atlantic, *Earth Planet Sci. Lett.*, 171, 149–156, 1999.

Claude-Ivanaj, C., A. W. Hofmann, I. Vlastélic, and A. Koschinsky, Recording changes in ENADW composition over the last 340 ka using high precision lead isotopes in a Fe-Mn crust, *Earth Planet Sci. Lett.*, 188, 73–89, 2001.

Cohen, A. S., R. K. O'Nions, R. Siegenthaler, and W. L. Griffin, Chronology of the pressure-temperature history recorded by a granulite terrain, *Contrib. Mineral. Petrol.*, 98, 303–311, 1988.

Damuth, J. E., and N. Kumar, Amazon cone: Morphology, sediments, age, and growth pattern, *Geol. Soc. Am. Bull.*, 86, 863–878, 1975.

Dobson, D. M., G. R. Dickens, and D. K. Rea, Terrigenous sedimentation on Ceara Rise, *Proc. Ocean Drill. Program Sci. Results*, 154, 465–474, 1997.

Dupré, B., J. Gaillardet, D. Rousseau, and C. J. Allègre, Major and trace elements of river-borne material: The Congo Basin, *Geochim. Cosmochim. Acta*, 60, 1301–1321, 1996.

Fischer, J., M. Rhein, F. Schott, and L. Stramma, Deep water masses and transports in the Vema Fracture Zone, *Deep Sea Res., Part I*, 43, 1067–1074, 1996.

Frank, M., Radiogenic isotopes: Tracers of past ocean circulation and erosional input, *Rev. Geophys*, 40(1), 1001, doi:10.1029/2000RG000094, 2002.

Frank, M., and R. K. O'Nions, Sources of Pb for Indian Ocean ferromanganese crusts: A record of Himalayan erosion?, *Earth Planet. Sci. Lett.*, 158, 121–130, 1998.

Frank, M., R. K. O'Nions, J. R. Hein, and V. K. Banakar, 60 Ma records of major elements and Pb-Nd isotopes from hydrogenous ferromanganese crusts: Reconstruction of seawater paleochemistry, *Geochim. Cosmochim. Acta*, 63, 1689–1708, 1999.

Frank, M., N. Whiteley, S. Kasten, J. R. Hein, and R. K. O'Nions, North Atlantic Deep Water export to the Southern Ocean over the past

14 Myr: Evidence from Nd and Pb isotopes in ferromanganese crusts, *Paleoceanography*, *17*(2), 1022, doi:10.1029/2000PA000606, 2002.

Galer, S. J. G., and W. Abouchami, Practical application of lead triple spiking for correction of instrumental mass discrimination, *Min. Mag.*, *62A*, 491–492, 1998.

Galer, S. J. G., and R. K. O'Nions, Chemical and isotopic studies of ultramafic inclusions from the San Carlos volcanic field, Arizona: A bearing on their petrogenesis, *J. Petrol.*, *30*, 1033–1064, 1989.

Goldstein, S. J., and S. B. Jacobsen, The Nd and Sr isotopic systematics of river water dissolved material: Implications for the sources of Nd and Sr in seawater, *Chem. Geol.*, *66*, 245–272, 1987.

Goldstein, S. L., R. K. O'Nions, and P. J. Hamilton, A Sm-Nd isotopic study of atmospheric dusts and particulates from major river systems, *Earth Planet. Sci. Lett.*, *70*, 221–236, 1984.

Goldstein, S. L., N. T. Arndt, and R. F. Stallard, The history of a continent from U-Pb ages of zircons from Orinoco River sand and Sm-Nd isotopes in Orinoco basin river sediments, *Chem. Geol.*, *139*, 271–286, 1997.

Grousset, F. E., P. E. Biscaye, A. Zindler, J. Prospero, and R. Chester, Neodymium isotopes as tracers in marine sediments and aerosols: North Atlantic, *Earth Planet. Sci. Lett.*, *87*, 367–378, 1988.

Grousset, F. E., P. Rognon, G. Coudé-Gaussen, and P. Pédemay, Origins of peri-Saharan dust deposits traced by their Nd and Sr isotopic composition, *Palaeogeogr. Palaeoclimatol. Palaeoecol.*, *93*, 203–212, 1992.

Grousset, F. E., M. Parra, A. Bory, P. Martinez, P. Bertrand, G. Shimmield, and R. M. Ellam, Saharan wind regimes traced by the Sr-Nd isotopic composition of subtropical Atlantic sediments: Last Glacial Maximum vs today, *Quat. Sci. Rev.*, *17*, 395–409, 1998.

Günther, D., I. Horn, and B. Hattendorf, Recent trends and developments in laser ablation-ICP-mass spectrometry, *Fresenius Z. Anal. Chem.*, *368*, 4–14, 2000.

Hamelin, B., F. E. Grousset, P. E. Biscaye, and A. Zindler, Lead isotopes in trade wind aerosols at Barbados: The influence of European emissions over the North Atlantic, *J. Geophys. Res.*, *94*, 16,243–16,250, 1989.

Hamelin, B., J. L. Ferrand, L. Alleman, E. Nicolas, and A. Veron, Isotopic evidence of pollutant lead transport from North America to the subtropical North Atlantic gyre, *Geochim. Cosmochim. Acta*, *61*, 4423–4428, 1997.

Henderson, G., and E. Maier-Reimer, Advection and removal of ^{210}Pb and stable Pb isotopes in the oceans: A general circulation model study, *Geochim. Cosmochim. Acta*, *66*, 257–272, 2002.

Henken-Mellies, W. U., J. Beer, F. Heller, K. J. Hsü, C. Shen, G. Bonani, H. J. Hofmann, M. Suter, and W. Wölfli, [10]Be and [9]Be in South Atlantic DSDP site 519: Relation to geomagnetic reversals and to sediment composition, *Earth Planet. Sci. Lett.*, *98*, 267–276, 1990.

Hoorn, C., J. Guerrero, G. A. Sarmiento, and M. A. Lorente, Andean tectonics as a cause for changing drainage patterns in Miocene northern South America, *Geology*, *23*, 237–240, 1995.

Jeandel, C., Concentration and isotopic composition of Nd in the Southern Atlantic Ocean, *Earth Planet. Sci. Lett.*, *117*, 581–591, 1993.

Jeandel, C., J. K. Bishop, and A. Zindler, Exchange of neodymium and its isotopes between seawater and small and large particles in the Sargasso Sea, *Geochim. Cosmochim. Acta*, *59*, 535–547, 1995.

Lacan, F., and C. Jeandel, Tracing Papua New Guinea imprint on the central equatorial Pacific Ocean using neodymium isotopic compositions and rare earth element patterns, *Earth Planet. Sci. Lett.*, *186*, 497–512, 2001.

Manheim, F. T., Marine cobalt resources, *Science*, *232*, 600–608, 1986.

McCartney, M. S., S. L. Bennett, and M. E. Woodgate-Jones, Eastward flow through the Mid-Atlantic Ridge at 11°N and its influence on the abyss of the eastern basin, *J. Phys. Oceanogr.*, *21*, 1089–1121, 1991.

McDaniel, D., S. M. McLennan, and G. N. Hanson, Provenance of Amazon fan muds: Constraints from Nd and Pb isotopes, *Proc. Ocean Drill. Program Sci. Results*, *155*, 169–176, 1997.

Measures, C. I., and S. Vink, On the use of dissolved aluminum in surface waters to estimate dust deposition to the ocean, *Global Biogeochem. Cycles*, *14*, 317–327, 2000.

Measures, C. I., T.-L. Ku, S. Luo, J. R. Southon, X. Xu, and M. Kusakabe, The distribution of [10]Be and [9]Be in the South Atlantic, *Deep Sea Res., Part I*, *43*, 978–1009, 1996.

Mercier, H., and P. Morin, Hydrography of the Romanche and Chain Fracture Zones, *J. Geophys. Res.*, *102*, 10,373–10,389, 1997.

Müller-Karger, F. E., C. R. McClain, T. R. Fisher, W. E. Esaias, and R. Varela, Pigment distribution in the Caribbean Sea: Observations from Space, *Prog. Oceanogr.*, *23*, 23–64, 1989.

Nesbitt, H. W., and G. M. Young, Sedimentation in the Venezuela Basin, circulation in the Caribbean Sea, and the onset of Northern Hemisphere glaciation, *J. Geol.*, *105*, 531–544, 1997.

O'Nions, R. K., M. Frank, F. von Blanckenburg, and H.-F. Ling, Secular variation of Nd and Pb isotopes in ferromanganese crusts from the Atlantic, Indian and Pacific Oceans, *Earth Planet. Sci. Lett.*, *155*, 15–28, 1998.

Paillet, J., M. Arhan, and M. S. McCartney, Spreading of Labrador Sea Water in the eastern North Atlantic, *J. Geophys. Res.*, *103*, 10,223–10,239, 1998.

Peterson, R. G., and L. Stramma, Upper-level circulation in the South Atlantic Ocean, *Prog. Oceanog.*, *26*, 1–73, 1991.

Piepgras, D. J., and S. B. Jacobsen, The isotopic composition of neodymium in the North Pacific, *Geochim. Cosmochim. Acta*, *52*, 1373–1381, 1988.

Piepgras, D. J., and G. J. Wasserburg, Isotopic composition of neodymium in waters from the Drake Passage, *Science*, *217*, 207–214, 1982.

Piepgras, D. J., and G. J. Wasserburg, Rare earth transport in the western North Atlantic inferred from isotopic observations, *Geochim. Cosmochim. Acta*, *51*, 1257–1271, 1987.

Piotrowski, A. M., D.-C. Lee, J. N. Christensen, K. W. Burton, A. N. Halliday, J. R. Hein, and D. Günther, Changes in erosion and ocean circulation recorded in the Hf isotopic compositions of North Atlantic and Indian Ocean ferromanganese crusts, *Earth Planet. Sci. Lett.*, *181*, 315–325, 2000.

Polzin, K. L., K. G. Speer, J. M. Toole, and R. W. Schmidt, Intense mixing of Antarctic Bottom Water in the equatorial Atlantic Ocean, *Nature*, *380*, 54–57, 1996.

Prospero, J. M., R. A. Glaccum, and R. T. Nees, Atmospheric transport of soil dust from Africa to South America, *Nature*, *289*, 570–572, 1981.

Rea, D. K., The paleoclimatic record provided by eolian deposition in the deep sea: The geologic history of wind, *Rev. Geophys.*, *32*, 159–195, 1994.

Reynolds, B. C., M. Frank, and R. K. O'Nions, Nd- and Pb- isotope time series from Atlantic ferromanganese crusts: Implications for changes in provenance and paleocirculation over the last 8 Myr, *Earth Planet. Sci. Lett.*, *173*, 381–396, 1999.

Rhein, M., L. Stramma, and G. Krahmann, The spreading of Antarctic bottom water in the tropical Atlantic, *Deep Sea Res., Part I*, *45*, 507–527, 1998.

Rognon, P., G. Coudé-Gaussen, M. Revel, F. E. Grousset, and P. Pédemay, Holocene Saharan dust deposition on the Cape Verde Islands: Sedimentological and Nd-Sr isotope evidence, *Sedimentology*, *43*, 359–366, 1996.

Romero, O. E., C. B. Lange, R. Swap, and G. Wefer, Eolian-transported freshwater diatoms and phytoliths across the equatorial Atlantic record: Temporal changes in Saharan dust transport patterns, *J. Geophys. Res.*, *104*, 3211–3222, 1999.

Rühlemann, C., B. Diekmann, S. Mulitza, and M. Frank, Late Quaternary changes of western equatorial Atlantic surface circulation and Amazon lowland climate recorded in Ceará Rise deep sea sediments, *Paleoceanography*, *16*, 293–305, 2001.

Rutberg, R. L., S. R. Hemming, and S. L. Goldstein, Reduced North Atlantic Deep Water flux to the glacial Southern Ocean inferred from neodymium isotope ratios, *Nature*, *405*, 935–938, 2000.

Schütz, L., Long range transport of desert dust with special emphasis on the Sahara, *Ann. N.Y. Acad. Sci.*, *338*, 515–532, 1980.

Spivack, A. J., and G. J. Wasserburg, Neodymium isotopic composition of the Mediterranean outflow and the eastern North Atlantic, *Geochim. Cosmochim. Acta*, *58*, 2767–2773, 1988.

Stordal, M. C., and G. J. Wasserburg, Neodymium isotopic study of Baffin bay water: Sources of REE from very old terranes, *Earth Planet. Sci. Lett.*, *77*, 259–272, 1986.

Sun, S. S., Lead isotopic study of young volcanic rocks from mid-ocean ridges, ocean islands and island arcs, *Philos. Trans. R. Soc. London, Ser. A*, *297*, 409–445, 1980.

Tachikawa, K., C. Jeandel, and B. Dupré, Distribution of rare earth elements and neodymium isotopes in settling particulate material of the tropical Atlantic Ocean (EUMELI site), *Deep Sea Res., Part I*, *44*, 1769–1792, 1997.

Tachikawa, K., C. Jeandel, and M. Roy-Barman, A new approach to the Nd residence time in the ocean: The role of atmospheric inputs, *Earth Planet. Sci. Lett.*, *170*, 433–446, 1999.

Tiedemann, R., M. Sarnthein, and R. Stein, Climatic changes in the western Sahara: Aeolo-marine sediment record of the last 8 million years (sites 657-661), *Proc. Ocean Drill. Program Sci. Results*, *108*, 241–261, 1989.

Vance, D., and K. W. Burton, Neodymium isotopes in planktonic foraminifera: A record of the response of continental weathering and ocean circulation rates to climate change, *Earth Planet. Sci. Lett.*, *173*, 365–379, 1999.

van de Flierdt, T., M. Frank, D.-C. Lee, and A. N. Halliday, Glacial weathering and the hafnium isotope composition of seawater, *Earth Planet. Sci. Lett.*, *198*, 167 – 175, 2002. (Correction, *Earth Planet. Sci. Lett.*, *201*, 639 – 647, 2002.)

van de Flierdt, T., M. Frank, A. N. Halliday, J. R. Hein, B. Hattendorf, D. Günther, and P. W. Kubik, Lead isotopes in North Pacific Deep Water—Implications for past changes in input sources and circulation patterns, *Earth Planet. Sci. Lett.*, *209*, 149 – 164, 2003.

von Blanckenburg, F., and T. F. Nägler, Weathering versus circulation-controlled changes in radiogenic isotope tracer composition of the Labrador Sea and Northern Atlantic Deep Water, *Paleoceanography*, *16*, 424 – 434, 2001.

von Blanckenburg, F., and R. K. O'Nions, Response of beryllium and radiogenic isotope ratios in Northern Atlantic Deep Water to the onset of northern hemisphere glacia-

tion, *Earth Planet. Sci. Lett.*, *167*, 175 – 182, 1999.

von Blanckenburg, F., R. K. O'Nions, N. S. Belshaw, A. Gibb, and J. R. Hein, Global distribution of beryllium isotopes in deep ocean water as derived from Fe-Mn crusts, *Earth Planet. Sci. Lett.*, *141*, 213 – 226, 1996a.

von Blanckenburg, F., R. K. O'Nions, and J. R. Hein, Distribution and sources of pre-anthropogenic lead isotopes in deep ocean water from Fe-Mn crusts, *Geochim. Cosmochim. Acta*, *60*, 4936 – 4957, 1996b.

Werner, M., I. Tegen, S. P. Harrison, K. E. Kohfeld, I. C. Prentice, Y. Balkanski, H. Rodhe, and C. Roelandt, Seasonal and interannual variability of the mineral dust cycle under present and glacial climate conditions, *J. Geophys. Res.*, *107*(D24), 4744, doi:10.1029/2002JD002365, 2002.

White, W., B. Dupré, and P. Vidal, Isotope and trace element geochemistry of sediments from the Barbados Ridge-Demerara Plain region,

Atlantic Ocean, *Geochim. Cosmochim. Acta*, *49*, 1875 – 1886, 1985.

———————————

M. Frank and A. N. Halliday, Institute for Isotope Geology and Mineral Resources, Department of Earth Sciences, ETH Zurich, ETH Zentrum, NO F51.3, Sonneggstrasse 5, CH-8092 Zurich, Switzerland. (frank@erdw.ethz.ch)

D. Günther and B. Hattendorf, Laboratory for Inorganic Chemistry, ETH Zurich, ETH Hönggerberg, HCI G 113, CH-8093 Zurich, Switzerland.

P. W. Kubik, Paul Scherrer Institute, c/o Institute for Particle Physics, ETH Zurich, ETH-Hönggerberg, CH-8093 Zurich, Switzerland.

T. van de Flierdt, Lamont Doherty Earth Observatory, Columbia University, 102 Geoscience Building (Office A), 61 Route 9W, Palisades, NY 10964, USA.